National Research Council Canada
Conseil national de recherches Canada

A NUMERICAL DETERMINATION OF THE BOW SHOCK WAVE IN TRANSONIC AXISYMMETRIC FLOW ABOUT BLUNT BODIES

BY

D.J. JONES, J.C. SOUTH, JR.

NATIONAL AERONAUTICAL ESTABLISHMENT

OTTAWA

MAY 1975

NRC NO. 14765

ISSN 0077-5541

AERONAUTICAL REPORT LR-586

A NUMERICAL DETERMINATION OF THE BOW SHOCK WAVE IN TRANSONIC AXISYMMETRIC FLOW ABOUT BLUNT BODIES

UNE DETERMINATION NUMERIQUE DE L'ONDE DE CHOC DE TETE AUTOUR DE CORPS EMOUSSES DANS UN ECOULEMENT TRANSONIQUE AXISYMETRIQUE

by/par

D.J. JONES*, J.C. SOUTH, JR.†

* Part of this work was carried out at NASA Langley where this author was on leave November 1973 — May 1974.

† NASA Langley

L.H. Ohman, Head/Chef
High Speed Aerodynamics Laboratory/
Laboratoire d'aérodynamique à hautes vitesses

F.R. Thurston
Director/Directeur

SUMMARY

A numerical method is developed for calculating axisymmetric transonic ($M > 1$) flow about a blunt body. The bow shock wave location is of particular interest. A Rankine Hugoniot jump is applied at the shock while relaxation on the isentropic equation of motion is used between shock and body. The shock wave is adjusted by a Newton type iteration scheme. Results are given for a sphere in the Mach number range 1.62 down to 1.02.

RESUME

Une méthode numérique est développée pour calculer l'écoulement transonique axisymétrique ($M > 1$) autour d'un corps émoussé. Le lieu et la forme de l'onde de tête revêt un intérêt particulier. Les équations de Rankine Hugoniot sont utilisées à la traversée de l'onde de tête et une méthode de relaxation est appliquée à l'équation isentropique du mouvement dans la couche de choc. La position du choc est réglée par la méthode itérative de Newton. Les résultats pour une sphère sont présentés pour des nombres de Mach allant de 1.62 à 1.02.

CONTENTS

TABLES

ILLUSTRATIONS

APPENDICES

SYMBOLS

Symbol	Definition
a	speed of sound
a, b	constants of the transformation (1)
A, B, C, D, E	coefficients in Equation (14), given by (16)
A', B', C'	constants of the transformation (2)
$A_0, A_1 \ldots$	coefficients used to define the shock shape
F	$r = F(\theta)$ is the equation of the shock wave
F(0)	the distance of the shock wave from the origin measured along the axis of symmetry. Thus shock stand-off distance = F(0) − 1.5 based on unit sphere radius
G	$r = G(\theta)$ is the equation of the body
i	numbers the lines τ = const (see Fig. 2)
j	numbers the lines η = const (see Fig. 2)
M	free stream Mach number
M_L	local Mach number
N	the line i = N (see Fig. 2) is the 'cutoff' line. Mesh size 5 × 10 implies N = 7
NSH	is the number of parameters used to define the shock wave i.e., $A_0, A_1, \ldots A_{NSH-1}$
P	the line j = P (see Fig. 2) refers to the shock wave. Mesh size 5 × 10 implies P = 12

SYMBOLS (Cont'd)

Symbol	Definition
p	pressure
r	polar co-ordinate, Figure 1
Q	a constant determining the amount of ϕ_{St} added, see (25)
q	velocity, $q^2 = u^2 + v^2$
R_i	residuals in the finite difference equations at the line next to the shock wave
S_1	$= \sum_{i=2}^{N} R_i^2$
S_2	$= \Sigma \Delta\phi_{ij}^2$
$\underline{t}$	vector tangent to the shock wave
U, V	velocity components given by (11)
$\bar{U}$, $\bar{V}$	velocity components given by (12)
u, v	velocity components in the r, θ directions
u', v'	velocity components in the η, τ plane
$\underline{V}$	velocity vector

Greek Letters

α, β	the coefficients of $-\phi_{St}$ and ϕ_{Nt} respectively
γ	ratio of specific heats, taken as 1.4
ΔM	required accuracy in Mach number measurements
$\Delta\eta, \Delta\tau$	mesh size in η, τ directions
Δt	a small increment in artificial time
Δ	distance shown on Figure 1
η, τ	transformed co-ordinates, see (2)
θ	polar co-ordinate

SYMBOLS (Cont'd)

Greek Letters	Definition
θ'	complement of the Mach angle
θ_0	shown in Figure 1
λ	determines the length of the Newton step
μ	angle between the lines η = const and θ = const
ξ, σ	transformed co-ordinates, see (1)
ϕ	velocity potential
ρ	density
σ_M	maximum value of σ, corresponding to $\theta = \pi/2$
ω	relaxation factor taken as 1.8

Subscripts

∞	refers to free stream
S	implies partial differentiation along the local streamline direction
N	implies partial differentiation along the direction normal to the local streamline
s	at the shock

A NUMERICAL DETERMINATION OF THE BOW SHOCK WAVE IN TRANSONIC AXISYMMETRIC FLOW ABOUT BLUNT BODIES

1.0 INTRODUCTION

For many years the problem of determining the bow shock wave location has been tackled by various authors. Several successful methods have resulted including the method of integral relations (Schemes I, II and III) of Belotserkovskiy (Ref. 4) and time dependent approaches such as Barnwell's (Ref. 3).

Belotserkovskiy used Schemes I and II, in which one of the independent variables is made discrete while the other is kept continuous, to compute solutions for flow about spheres and other shapes and was successful in computing flow characteristics for Mach numbers ranging from hypersonic down to about 1.5. For Mach numbers lower than this convergence was difficult to obtain so he devised Scheme III in which both independent variables were discretized and dependent variables were represented by polynomials. In this way solutions could be obtained for Mach numbers down to 1.05.

Barnwell's method, which in general will treat bodies with discontinuous slope as well as bodies at incidence, starts from an assumed shock wave and integrates the time dependent equations of motion until a steady state is reached. Solutions can be obtained efficiently for Mach numbers as low as about 1.3 but below this the method may produce kinky shocks or else is very time consuming. For example another time dependent method due to Aungier (Ref. 9) took 16 hours to compute the flow about a hemisphere cylinder at $M = 1.1$ on an IBM 370/155 (quoted in Ref. 10).

Since Scheme III seemed the most applicable method to the transonic regime it was first decided to use the collocation method of Jurak et al (Ref. 6) which is similar to Scheme III. By this method results were obtained for M as low as 1.1 but even here convergence was slow and the results for $M < 1.5$ did not compare too well with experimental data. Even the Scheme III results given by Belotserkovskiy and shown on Figure 6 do not look sufficiently accurate.

In view of these shortcomings of other techniques it was decided to attempt a relaxation solution of the full potential equation for inviscid steady transonic flow. In this equation the flow is assumed to be irrotational and hence isentropic. However, the shock is treated as a discontinuity and either Rankine Hugoniot jump relations or isentropic jump conditions (neglecting momentum conservation) are used. Use of the Rankine Hugoniot conditions, applied to flow about spheres, gives shock locations which compare reasonably well with experiment at Mach numbers 1.17, 1.30 and 1.62. Experiments at lower Mach numbers will be made at NAE in the near future.

As this paper was in preparation the work of Frank and Zeirep (Ref. 11) came to the authors' attention. In this work they give a semi empirical formula for stand-off distance which is obtained by modifying a formula derived for slender bodies of revolution. Generally their prediction of stand-off distance is significantly greater than our prediction.

The first section to follow briefly describes the preliminary attempts made to solve the problem. Thereafter the paper is concerned with the potential approach. We first develop, following Jameson (Ref. 1), the finite difference scheme and analyse its stability. Then the shock representation and shock jumps are considered. Finally the two stage iteration procedure, one for the shock and one for relaxation of the interior equations is considered.

2.0 PRELIMINARY ATTEMPTS

Several numerical methods for the calculation of the bow shock were tried. They included the time dependent approach (Ref. 3), a collocation method similar to Scheme III of the method of integral relations (Ref. 4) and the method of lines as described in Reference 5.

In the time dependent method a flow field and shock wave are assumed and these are adjusted whilst marching forward in time until a steady state is reached. Good results can be obtained in this way for higher Mach numbers but at M less than about 1.3 convergence is slow and the shock wave is not smooth.

The collocation method, used in Reference 6 at M = 10, (this is similar to Scheme III of the method of integral relations, Ref. 4) was next attempted. The stand-off distance was found to be reasonably good for $M \geqslant 1.5$.

Finally a method of lines solution was attempted and this gave reasonable results for $M \geqslant 1.3$ although even at this Mach number convergence was slow (Ref. 7).

Some results of these computations are shown in Figure 6, where we show a logarithm of stand-off distance against a logarithm of Mach number. Since these preliminary attempts gave such poor results at the lower Mach numbers it was decided to assume the flow irrotational and use the potential equation.

3.0 EQUATION OF MOTION AND THE BOUNDARY CONDITIONS

3.1 The Region of Computation

Referring to Figure 1, O is the origin of the spherical polar co-ordinate system (r, θ) set back a distance d from the leading edge of the body. ODC is the line of symmetry $\theta = 0$ and OAB is the " cutoff" line $\theta = \pi/2$. AD is the axisymmetric body and BC is the stand-off shock wave. Then the region of computation is ABCD.

In Figure 1 we draw a general ellipsoid although we confine our attention to spheres in the results section. In this case we take unit radius and set $d = 1.5, \Delta = 0.5$.

3.2 Transformations

Let $r = G(\theta)$ and $r = F(\theta)$ be the equations of body and shock respectively.

In order to fix the shock and body as co-ordinate lines let us introduce new variables (ξ, σ) such that

$$\xi = \frac{r - G(\theta)}{F(\theta) - G(\theta)} \qquad \theta = a\sigma^3 + b\sigma \tag{1}$$

The region of computation is therefore $0 \leqslant \xi \leqslant 1, 0 \leqslant \sigma \leqslant \sigma_M$, where σ_M corresponds to $\theta = \pi/2$ (the determination of a, b and σ_M is shown in Appendix A).

The above system of co-ordinates could be used as it stands. However one should notice that at Mach numbers approaching unity the shock wave is many body radii from the axis (especially AB $\gg$ AO in Fig. 1) and while flow quantities do not change greatly at distances greater than two or three radii from the axis they do change considerably on approaching the body. Thus a transformation which puts more co-ordinate lines near the body is desirable. Such a transformation is

$$\xi = A'\eta + B'\eta^3 + C'\eta^4 \qquad \tau = \sigma \tag{2}$$

where A', B', C' are chosen as shown in Appendix B.

The transformation of the equation of motion which is to follow will be effected by the formulas

$$\frac{\partial}{\partial r} = \xi_r \frac{\partial}{\partial \xi}; \quad \frac{\partial}{\partial \theta} = \sigma_\theta \frac{\partial}{\partial \sigma} + \xi_\theta \frac{\partial}{\partial \xi}$$

$$\frac{\partial^2}{\partial r^2} = \xi_r^2 \frac{\partial^2}{\partial \xi^2}; \quad \frac{\partial^2}{\partial r \partial \theta} = \xi_{r\theta} \frac{\partial}{\partial \xi} + \xi_\theta \xi_r \frac{\partial^2}{\partial \xi^2} + \sigma_\theta \xi_r \frac{\partial^2}{\partial \xi \partial \sigma} \tag{3}$$

$$\frac{\partial^2}{\partial \theta^2} = \xi_{\theta\theta} \frac{\partial}{\partial \xi} + \sigma_{\theta\theta} \frac{\partial}{\partial \sigma} + \xi_\theta^2 \frac{\partial^2}{\partial \xi^2} + \sigma_\theta^2 \frac{\partial^2}{\partial \sigma^2} + 2\sigma_\theta \xi_\theta \frac{\partial^2}{\partial \xi \partial \sigma}$$

where

$$\xi_r = \frac{1}{F - G} \quad \xi_\theta = -\xi_r (G' + \xi(F' - G'))$$

$$\xi_{r\theta} = -\xi_r^2 (F' - G')$$

$$\xi_{\theta\theta} = -\xi_{r\theta} (G' + \xi(F' - G')) - \xi_r (G'' + \xi(F'' - G'') + \xi_\theta (F' - G')) \tag{4}$$

$$\sigma_\theta = (3a\sigma^2 + b)^{-1}$$

$$\sigma_{\theta\theta} = -\theta_{\sigma\sigma}/\theta_\sigma^3$$

and by

$$\frac{\partial}{\partial \xi} = \eta_\xi \frac{\partial}{\partial \eta} \qquad \frac{\partial^2}{\partial \xi^2} = \eta_{\xi\xi} \frac{\partial}{\partial \eta} + \eta_\xi^2 \frac{\partial^2}{\partial \eta^2}$$

where (5)

$$\eta_\xi = 1/\xi_\eta \text{ and } \eta_{\xi\xi} = -\xi_{\eta\eta}/\xi_\eta^3$$

3.3 The Equation of Motion

In spherical co-ordinates (r, θ) shown in Figure 1, the equation of motion is a^2 div $\underline{V} = \underline{V} \cdot$ grad $(\frac{1}{2}V^2)$ where $\underline{V} = (u, v)$ and a^2 is given by

$$u^2 + v^2 + \frac{2}{\gamma - 1} a^2 = V_\infty^2 + \frac{2}{\gamma - 1} a_\infty^2 \cdot \tag{6}$$

We assume the flow is isentropic, thus irrotational so that curl $\underline{V} = 0$ and hence we can define a disturbance potential ϕ by $\underline{V} = \underline{V}_\infty + \nabla\phi$ where $\underline{V}_\infty$ is the free stream velocity vector. Making the appropriate substitutions into (6) gives an equation for ϕ:

$$\left(1 - \frac{u^2}{a^2}\right) \phi_{rr} - \frac{2uv}{a^2 r} \phi_{r\theta} + \left(1 - \frac{v^2}{a^2}\right) \frac{\phi_{\theta\theta}}{r^2}$$

$$= -\left(2 - \frac{v^2}{a^2}\right) \frac{\phi_r}{r} - \left(\frac{2uv}{a^2} + \cot\theta\right) \frac{\phi_\theta}{r^2} \tag{7}$$

as long as $\theta \neq 0$. If $\theta = 0$, (7) becomes

$$\left(1 - \frac{u^2}{a^2}\right) \phi_{rr} + \frac{2\phi_{\theta\theta}}{r^2} = -\frac{2\phi_r}{r} \cdot \tag{8}$$

In these equations a^2 is given by

$$a^2 = a_\infty^2 + \frac{\gamma - 1}{2} \left\{ V_\infty^2 - u^2 - v^2 \right\} \tag{9}$$

where

$$u = -V_\infty \cos\theta + \phi_r$$

$$v = V_\infty \sin\theta + \frac{1}{r} \phi_\theta \tag{10}$$

Rather than make the substitution of transformation (3, 4, 5) directly into (7) we first consider the equation written in a form suitable for application of Jameson's rotated difference scheme (Ref. 1).

For this scheme we need to write the principal part of Equation (7) as

$$\left(1 - \frac{q^2}{a^2}\right) \phi_{SS} + \phi_{NN}$$

where S is the local streamline direction at the mesh point and N is normal to the streamline; the subscripts refer to partial differentiation in the appropriate direction. Now we have by definition

$$q \frac{\partial}{\partial S} = u \frac{\partial}{\partial r} + \frac{v}{r} \frac{\partial}{\partial \theta}$$

$$= U \frac{\partial}{\partial \eta} + V \frac{\partial}{\partial \tau}$$

where

$$U = \left(u\xi_r + \frac{v}{r}\ \xi_\theta \right) \eta_\xi \qquad \text{and } V = \frac{v}{r} \tag{11}$$

(N.B. U and V are important physically as their sign indicates the direction of flow in the (η, τ) plane as shown in Appendix C), and also

$$q\ \frac{\partial}{\partial N} = -v\ \frac{\partial}{\partial r} + \frac{u}{r}\ \frac{\partial}{\partial \theta}$$

$$= -\overline{V}\ \frac{\partial}{\partial \eta} + \overline{U}\ \frac{\partial}{\partial \tau}$$

where

$$\overline{V} = \left(v\xi_r - \frac{u}{r}\ \xi_\theta \right) \eta_\xi \qquad \text{and } \overline{U} = \frac{u}{r}\ \sigma_\theta \tag{12}$$

Therefore

$$q^2\ \frac{\partial^2}{\partial S^2} = U^2\ \frac{\partial^2}{\partial \eta^2} + 2UV\ \frac{\partial^2}{\partial \eta \partial \tau} + V^2\ \frac{\partial^2}{\partial \tau^2}$$

$$q^2\ \frac{\partial^2}{\partial N^2} = \overline{V}^2\ \frac{\partial^2}{\partial \eta^2} - 2\overline{U}\overline{V}\ \frac{\partial^2}{\partial \eta \partial \tau} + \overline{U}^2\ \frac{\partial^2}{\partial \tau^2} \tag{13}$$

Transforming (7, 8) to the (ξ, σ) co-ordinates gives

$$\theta \neq 0: \quad A\phi_{\xi\xi} + B\phi_{\xi\sigma} + C\phi_{\sigma\sigma} + D\phi_\xi + E\phi_\sigma = 0$$

$$\theta = 0: \quad \left(1 - \frac{u^2}{a^2}\right) \xi_r^2 \phi_{\xi\xi} + \frac{2}{r^2}\ \phi_{\sigma\sigma} + 2\phi_\xi \left(\frac{\xi_{\theta\theta}}{r^2} + \frac{\xi_r}{r} \right) = 0 \tag{14}$$

and transformation to (η, τ) gives

$$A\eta_\xi^2 \phi_{\eta\eta} + \eta_\xi B\phi_{\eta\tau} + C\phi_{\tau\tau} + \left(A\eta_{\xi\xi} + \eta_\xi D \right) \phi_\eta + E\phi_\tau = 0 \tag{15a}$$

$$\left(1 - \frac{u^2}{a^2}\right) \xi_r^2 \left(\eta_{\xi\xi}\phi_\eta + \eta_\xi^2 \phi_{\eta\eta} \right) + \frac{2}{r^2}\ \sigma_\theta^2 \phi_{\tau\tau} + 2\eta_\xi \phi_\eta \left(\frac{\xi_{\theta\theta}}{r^2} + \frac{\xi_r}{r} \right) = 0 \tag{15b}$$

where

$$A = \left(1 - \frac{u^2}{a^2}\right) \xi_r^2 - \frac{2uv}{a^2 r} \xi_r \xi_\theta + \frac{\xi_\theta^2}{r^2} \left(1 - \frac{v^2}{a^2}\right) \tag{16a}$$

$$B = \frac{2}{r^2} \sigma_\theta \xi_\theta \left(1 - \frac{v^2}{a^2}\right) - \frac{2uv}{a^2 r} \sigma_{\xi} \xi_r \tag{16b}$$

$$C = \sigma_\theta^2 \left(1 - \frac{v^2}{a^2}\right) \Big/ r^2 \tag{16c}$$

$$D = \left(2 - \frac{v^2}{a^2}\right) \frac{\xi_r}{r} + \left(\frac{2uv}{a^2} + \cot\theta\right) \frac{\xi_\theta}{r^2} + \left(1 - \frac{v^2}{a^2}\right) \frac{\xi_{\theta\theta}}{r^2} - \frac{2uv}{a^2 r} \xi_{r\theta} \tag{16d}$$

$$E = \left(1 - \frac{v^2}{a^2}\right) \sigma_{\theta\theta} / r^2 + \left(\frac{2uv}{a^2} + \cot\theta\right) \sigma_\theta / r^2 \tag{16e}$$

Now (15a) can be written

$$\left(1 - \frac{q^2}{a^2}\right) \phi_{SS} + \phi_{NN} + \left(A\eta_{\xi\xi} + D\eta_\xi\right) \phi_\eta + E\phi_\tau = 0 \tag{17}$$

as shown in Appendix D. Equation (15b), applied only at $\tau = 0$, is left in the given form since the flow is obviously in the η direction.

3.4 Boundary Conditions

(i) On the body the normal velocity is zero. Thus

$$u = v \frac{G'}{G}$$

hence

$$\xi_r \phi_\xi = \frac{1}{r} \left(\xi_\theta \phi_\xi + \sigma_\theta \phi_\sigma\right) \frac{G'}{G} + v_\infty \frac{G'}{G} - u_\infty$$

and so

$$\left(\xi_r - \frac{G'}{G^2} \xi_\theta\right) \eta_\xi \phi_\eta = \sigma_\theta \phi_\tau \frac{G'}{G^2} + v_\infty \frac{G'}{G} - u_\infty \tag{18}$$

giving ϕ_η on the body ($\eta = 0$).

(ii) Line of Symmetry

In this case we introduce an image line ($\tau = -\Delta\tau$) and make the potential symmetric.

(iii) Along AB

There is no boundary condition given at the cutoff line so we can only assume that ϕ is well behaved in this region (no shocks). Then we can introduce a line $\tau = \tau_{MAX} + \Delta\tau$ and extrapolate quadratically to this line from the values of ϕ at τ_{MAX}, $\tau_{MAX} - \Delta\tau$ and $\tau_{MAX} - 2\Delta\tau$.

(iv) Equations at the Shock Wave

At the shock ($\eta = \xi = 1$) we apply the Rankine Hugoniot (R-H) conditions expressing continuity of tangential velocity, energy, mass, and momentum. These are written as

$$v + \frac{F'}{F} u = v_\infty + \frac{F'}{F} u_\infty \tag{19a}$$

$$\rho V_n = \rho_\infty V_{n_\infty} \tag{19b}$$

$$p + \rho V_n^2 = p_\infty + \rho_\infty V_{n_\infty}^2 \tag{19c}*$$

$$\frac{\gamma}{\gamma - 1} \frac{p}{\rho} + \tfrac{1}{2} V_n^2 = \frac{\gamma}{\gamma - 1} \frac{p_\infty}{\rho_\infty} + \tfrac{1}{2} V_{n_\infty}^2 \tag{19d}$$

where

$$V_n = \frac{u - v \dfrac{F'}{F}}{\sqrt{1 + \dfrac{F'^2}{F^2}}}$$

These equations are solved for u, v, p and ρ. In particular u is needed to provide boundary conditions for ϕ as shown below.

Firstly we can show that ϕ is constant along the shock. We know that $\underline{V} \cdot \underline{t} = \underline{V}_\infty \cdot \underline{t}$ because of continuity of tangential velocity. But $\underline{V} = \underline{V}_\infty + \nabla\phi$ and so $\nabla\phi \cdot \underline{t} = 0$ or $\partial\phi/\partial t = 0$. Hence ϕ is constant along the shock. If we define the constant (which is arbitrary) to be zero then we have

$$\phi = 0 \text{ at } \eta = 1 \tag{20}$$

We also know the R-H value of u at the shock (u_s say) by solving (19), and hence we have

$$u_s = u_\infty + \phi_r$$

$$= u_\infty + \xi_r \eta_\xi \phi_\eta$$

or

$$\phi_\eta = \frac{u_s - u_\infty}{\xi_r \eta_\xi} \tag{21}$$

---

* We could omit this equation and use $p/\rho^\gamma = p_\infty/\rho_\infty{}^\gamma$ for the isentropic shock relation.

4.0 NUMERICAL PROCEDURE

4.1 Relaxation

Consider the computational grid shown in Figure 2. Referring to Equations (17) and (15b) we write the first derivatives as

$$\phi_\eta = \frac{\phi_{i,j+1} - \phi_{i,j-1}}{2\Delta\eta}$$

$$\phi_\tau = \frac{\phi_{i+1,j} - \phi_{i-1,j}}{2\Delta\tau}$$

while second derivatives are written in central difference form if the flow is subsonic ($q^2 < a^2$) or in backward difference form for ϕ_{SS} if $q^2 > a^2$, as follows.

(i) Subsonic, $q^2 < a^2$

Following Jameson (Ref. 1) we use

$$\phi_{\eta\eta} = \frac{\phi^+_{i,j+1} - 2\phi^+_{i,j} + \phi^+_{i,j-1}}{\Delta\eta^2} \tag{22a}$$

$$\phi_{\eta\tau} = \frac{\phi^+_{i-1,j-1} - \phi^+_{i-1,j+1} - \phi_{i+1,j-1} + \phi_{i+1,j+1}}{4\Delta\eta\Delta\tau} \tag{22b}$$

$$\phi_{\tau\tau} = \frac{\phi^+_{i-1,j} - \frac{2}{\omega}\phi^+_{i,j} - 2\left(1 - \frac{1}{\omega}\right)\phi_{i,j} + \phi_{i+1,j}}{\Delta\tau^2}$$

for all the second derivatives terms, where ω is the over-relaxation factor and is taken as 1.8 in the present calculations. The superscript + implies that new values are to be computed (for i subscript) or used (for i-1 subscript) in the iteration process, otherwise values of ϕ from the previous step are used.

Thus in the subsonic region we have a tridiagonal system of equations for $\phi^+_{i,j+1}$, $\phi^+_{i,j}$ and $\phi^+_{i,j-1}$ to be solved at each step of the line relaxation procedure.

(ii) Supersonic $q^2 > a^2$

Considering $(1 - q^2/a^2)\,\phi_{SS} + \phi_{NN}$ we use (22a) and (22b) for the $\phi_{\eta\eta}$ and $\phi_{\eta\tau}$ contributions to ϕ_{NN} while for $\phi_{\tau\tau}$ in the ϕ_{NN} expression we use

$$\phi_{\tau\tau} = \frac{\phi^+_{i-1,j} - \phi^+_{i,j} - \phi_{i,j} + \phi_{i+1,j}}{\Delta\tau^2}$$

For contributions to ϕ_{SS} we use all old values of ϕ as follows

$$\phi_{\eta\eta} = \frac{\phi_{i,j} - 2\phi_{i,j\mp1} + \phi_{i,j\mp2}}{\Delta\eta^2}$$

$$\phi_{\eta\tau} = \pm \frac{\left(\phi_{i,j} - \phi_{i,j\mp1} - \phi_{i-1,j} + \phi_{i-1,j\mp1}\right)}{\Delta\eta\Delta\tau}$$

$$\phi_{\tau\tau} = \frac{\phi_{i,j} - 2\phi_{i-1,j} + \phi_{i-2,j}}{\Delta\tau^2}$$

where the upper sign is used if $U > 0$ and the lower sign if $U < 0$. These formulas give a finite difference representation consistent with the flow direction since U is proportional to the velocity in the τ = const direction and V is porportional to the velocity in the η = const direction (see Appendix C).

Now to investigate convergence in the same manner as Jameson (Ref. 1) we have to introduce an artificial time into the difference equations so that for instance

$$\phi^{+}_{ij} = \phi_{ij} + \Delta t \frac{\partial \phi_{ij}}{\partial t}$$

Then in ϕ_{NN} we have

$$\phi_{NN}^{(\text{OLD VALUES})} + \frac{\Delta t}{\Delta\tau}\frac{\bar{U}}{q^2}\left(\bar{V}\phi_{\eta t} - \bar{U}\phi_{\tau t}\right) = \phi_{NN}^{(\text{OLD VALUES})} - \frac{\Delta t}{\Delta\tau}\frac{\bar{U}}{q}\phi_{Nt} \qquad (23)$$

while in ϕ_{SS}, since all old values are used, there is no ϕ_{St} contribution. Therefore we must artificially add some ϕ_{St} to the finite difference equation so that we satisfy Jameson's necessary condition for convergence (see Ref. 1 for full details) i.e.

$$\alpha^2 > \beta^2\left(M_L^2 - 1\right) \qquad (24)$$

where M_L is the local Mach number and $-\alpha$ and β are the coefficients of ϕ_{St} and ϕ_{Nt} respectively; in our case $\beta = -\bar{U}/q \cdot \Delta t/\Delta\tau$ (see (23)).

Now

$$\phi_{St} = \frac{U}{q}\phi_{\eta t} + \frac{V}{q}\phi_{\tau t}$$

which can be written in finite difference form as

$$\pm \frac{U}{q}\left(\frac{\phi^+_{i\,j} - \phi^+_{i,\,j\mp1} - \phi_{ij} + \phi_{i,\,j\mp1}}{\Delta\eta\Delta t}\right)$$

$$+ \frac{V}{q}\left(\frac{\phi^+_{i\,j} - \phi^+_{i-1,\,j} - \phi_{ij} + \phi_{i-1,\,j}}{\Delta\tau\Delta t}\right)$$

with the upper signs used if $U > 0$, otherwise lower signs (since U indicates the flow direction). Thus the appropriate amount of ϕ_{St} to be added is

$$Q \cdot \frac{|\bar{U}|}{q}\frac{\Delta t}{\Delta\tau}\,\phi_{St}$$

where

$$Q^2 > M_L^2 - 1 \tag{25}$$

to meet condition (24). Since we are dealing with transonic flows, by experience we can expect M_{max} to be about three so that choosing $|Q| = 4$ should be sufficient. As to the sign of Q it should be chosen so that diagonal dominance of the tri-diagonal equations is enhanced as follows.

The coefficient of $\phi^+_{i,\,j-1}$ is

$$\frac{\bar{V}^2}{q^2\Delta\eta^2} - \frac{QU\,|\bar{U}|}{q^2\Delta\tau\Delta\eta}$$

$$(U > 0)$$

the coefficient of $\phi^+_{i,\,j+1}$ is

$$\frac{\bar{V}^2}{q^2\Delta\eta} + \frac{Q\,|\bar{U}|\,U}{q^2\Delta\tau\Delta\eta}$$

$$(U < 0)$$

and the coefficient of $\phi^+_{i,\,j}$ is

$$\frac{-2\bar{V}^2}{q^2\Delta\eta^2} - \frac{\bar{U}^2}{q^2\Delta\tau^2} + \frac{Q\,|U|\,|\bar{U}|}{q^2\Delta\tau\Delta\eta} + \frac{Q\,|\bar{U}|\,V}{q^2\Delta\tau^2}$$

Clearly $Q < 0$ is required since then the magnitude of the diagonal term will be enlarged (unless V ($= \sigma_\theta\, v/r$) is negative in which case the flow direction is clearly wrong). In practice a test is always made to ensure that the system is diagonally dominant; if it is not an error message is printed and computation ceases. This dominance is necessary to ensure a well behaved solution to the system of algebraic equations.

Unfortunately this process does not give convergent results. As an example of the divergence we took the converged solution for M = 1.3, P = 12, N = 7 (i.e. 5 X 10 mesh) and inspected $\Sigma\Delta\phi_{i\,j}^2$ on successive iterations. On the first iteration $\Sigma\Delta\phi_{i\,j}^2$ was 10.59, on the second 67.5 and then no diagonal dominance was present on the next iteration.

In order to gain some insight into the amount of ϕ_{St} to be added to give convergence we next looked at the amplification factor, G, given by

$$G = \frac{\phi_{i\,j}^{+}}{\phi_{i\,j}}$$

In Appendix E we show that $|G|$ is less then unity in a simplified case where $\bar{U} = U$, $\bar{V} = V$ and $U^2 + V^2 = q^2$, provided

$$\alpha \geqslant q \frac{\Delta t}{\Delta \tau} M_L^2$$

In practice, however, using $\alpha = q\ \Delta t/\Delta\tau\ M_L^2$ did not give convergence and we finally had to use

$$\alpha = q \frac{\Delta t}{\Delta \tau} M_L^2 \left[5 + \frac{50}{3} (M-1)\right]$$

to give convergence. Cases which were very slow to converge were those in which M was close to unity. This is probably due to the 'cutoff' line, AB in Figure 1, lying partially in the subsonic part of the flow field. Table 1 illustrates the convergence when M = 1.02 by listing $\Sigma\Delta\phi_{i,\,j}^2$ on successive iterations. Compare this to the M = 1.3 case shown in Table 2. It can be seen that at M = 1.02 the convergence is much slower. Since convergence is slow at the lower Mach numbers fine grids are not computed in these cases.

4.2 Finite Difference Application of the Boundary Conditions

Referring to the boundary conditions in Section 3.4 we now write them in finite difference form.

(i) To apply (18) at $\eta = 0$ we introduce a line of points at $\eta = -\Delta\eta$ and write ϕ_η as

$$\frac{\phi_{i,\,3} - \phi_{i,\,1}}{2\Delta\eta}$$

while ϕ_τ is calculated as

$$\frac{\phi_{i+1,\,2} - \phi_{i-1,\,2}}{2\Delta\tau}$$

Substitution into (18) then gives values for $\phi_{i,\,1}$.

(ii) From symmetry

$$\phi_{1,\,j} = \phi_{3,\,j}$$

(iii) By quadratic extrapolation

$$\phi_{N+1,\,j} = 3\left(\phi_{N,\,j} - \phi_{N-1,\,j}\right) + \phi_{N-2,\,j}$$

(iv) $\phi_{i,\,P} = 0$. We also need $\phi_{i,\,P-1}$ from the shock boundary conditions. Now we know ϕ_η from (21) thus we could write

$$\phi_\eta = \frac{\phi_{i,\,P} - \phi_{i,\,P-1}}{\Delta\eta}$$

and accordingly find $\phi_{i,\,P-1}$. However, the above formula is only first order accurate for the first derivative whilst we really require second order accuracy for consistency with the finite difference equations used in the elliptic region. We obtain second order accuracy by using the equation of motion (15) to find $\phi_{\eta\eta}$ at the shock wave $\left(\phi^s_{\eta\eta}\right.$ say$\left.\right)$.

Then we have

$$\phi_{i,\,P-1} = \phi_{i,\,P} - \Delta\eta\phi^s_\eta + \frac{\Delta\eta^2}{2}\,\phi^s_{\eta\eta} \tag{26}$$

giving, in effect, second order accuracy for the finite difference representation of ϕ_η at the shock.

Having seen how to apply the boundary conditions (once a shock shape has been estimated) we can now iterate, by relaxation, the equation of motion written in finite difference form.

4.3 The Inner Loop Iteration

The preceding describes the finite difference representation of the equations of motion and the boundary conditions. To drive the residuals in these equations smaller we solve for $\phi^+_{i,\,j}$ starting with line i = 2 (the line of symmetry) and proceeding to line i = N. On each line we solve for $\phi^+_{i,\,j}$ (j = 2 . . . P-2 inclusive) by solving the appropriate tridiagonal system of equations. Values for $\phi^+_{i-1,\,j}$ are known except at the line i = 2 and here we are forced to use old values.

Thus we have a technique for driving residuals smaller at the points i = 2 . . . N, j = 2 . . . P-2 once $\phi_{i,\,P-1}$ are fixed. The next section describes how an outer iteration is used to improve the shock shape and hence $\phi_{i,\,P-1}$ (from (26)) so that the residuals at j = P-1 are made smaller.

4.4 Newton Iteration of the Shock Wave — The Outer Loop

We have shown how $\phi_{i,\,P-1}$ is obtained (26) from the shock wave relations and also we have shown how the values of ϕ in the rest of the flow field, assuming $\phi_{i,\,P-1}$ is computed from (26), are obtained. However we still have to iterate so that the shock wave $r = F(\theta)$ is adjusted to the hopefully correct position. To make the adjustment we must have some outstanding equations still to be satisfied. Clearly these equations are the finite difference form of the equation of motion written at each point at the line next to the shock wave, i.e. j = P-1, i = 2 . . . N. Unfortunately, these equations cannot be written in backward difference form in the supersonic region since we only have values available at one mesh line further upstream — thus a central difference form has to be used even in the supersonic region. This, however, will not affect convergence since a Newton method is to be used on this line to drive the equation residuals, R_i (i = 2 . . . N), smaller by adjusting the parameters which define the shock wave. These parameters A_j (j = 0, 1 . . . NSH-1) are defined in the next subsection. In the outer iteration the parameters A_j are changed by an amount $\lambda\delta A_j$ where δA_j is given by

$$\sum_{j=0}^{NSH-1} \left\{ \sum_{k=2}^{N} \frac{\partial R_k}{\partial A_i} \frac{\partial R_k}{\partial A_j} \right\} \delta A_j = - \sum_{k=2}^{N} R_k \frac{\partial R_k}{\partial A_i} \qquad i = 0, 1 \ldots NSH-1$$

The above is the Newton step to minimize $S_1 = \sum_{i=2}^{N} R_i^2$ with respect to A_j . λ $(0 < \lambda \leqslant 1)$ is chosen so that S_1 decreases (normally $\lambda = 1$ but may have to be smaller to ensure a decrease in S_1). The partial derivatives in the above equation are found by differences using a perturbation to A_j of 10^{-4}.

4.4.1 Form of the Shock Wave

We could let the shock wave $r = F(\theta)$ be defined by its values $F(\theta_2), F(\theta_3) \ldots F(\theta_N)$. However there are two reasons against this form. This first reason is for efficiency — if we can define the shock by less than N parameters then the Newton iteration of the shock is computationally quicker. More importantly, though, the finite differences approximations to determine $F'(\theta)$ and $F''(\theta)$ will be poor in the region near $\theta = 90°$ because, here, there are large gradients of F since F is going rapidly to infinity at the lower Mach numbers. Thus it is important to have an analytic form for the shock that can be differentiated analytically.

Such a form is given by

$$r = F(\theta) = \frac{1 - \cos\theta'}{\cos\theta - \cos\theta'} \sum_{0}^{NSH-1} A_n \theta^{2n}$$

where θ' is the complement of the Mach angle. This has the correct form since such a shock wave is asymptotic to the Mach line and is also symmetrical as required by the problem. Note that F (0) gives the stand-off distance except for a constant which depends on the location of the origin of the co-ordinate system. In the cases computed, this origin is chosen such that $\Delta = \frac{1}{2}DE$ (see Fig. 1) where E is the centre of the sphere.

4.5 Iteration Procedure

In the iteration procedure described previously the inner loop drives $S_2 = \Sigma \Delta \phi_{ij}^2$ smaller by relaxation while the outer loop adjusts the shock shape so that residuals R_i at the line next to the shock are driven smaller. One problem in this scheme is knowing when to adjust the shock shape — if we adjust it when S_2 is still large then the adjustment may be completely meaningless while on the other hand if we wait until S_2 is too small the efficiency of the scheme suffers. Thus it was decided that the shock would not be adjusted until S_2 was less than $P \cdot N \cdot 10^{-4}$. Also to avoid possibly meaningless changes to shock position a change in F (0) of greater than 0.05 on each step was not allowed. Likewise for efficiency a change in F (0) of less than 0.001 was not made. A typical iteration is shown in Table 3 at M = 1.3, mesh size 5 × 10, i.e. N = 7 and P = 12, and ϕ_{ij} set to zero initially.

A flow diagram of the iteration scheme is shown in Figure 3.

5.0 SOME PROGRAM DETAILS

5.1 Initial Estimates

We first selected M = 1.3 as a starting Mach number, made a rough estimate of the coefficients that form the shock, set $\phi_{ij} = 0$ on a 5 × 10 mesh and let the process run. Having obtained this solution we then used the results to give the estimates for the Mach numbers 1.17 and 1.10.

Having obtained these solutions we then extrapolated quadratically the shock coefficients and the initial ϕ_{ij} down to lower Mach numbers. In this way solutions were obtained for M = 1.08, 1.06, 1.05, 1.04, 1.03 and 1.02. At some of these Mach numbers finer grids (10 X 20 and 20 X 40) were computed. To get estimates for the finer grids we used the same shock values from the coarser grid and interpolated ϕ_{ij} linearly to obtain values at the extra mesh points.

5.2 Computer Time

The three meshes 5 X 10, 10 X 20 and 20 X 40 took approximately six minutes on an IBM 360/67 for the M = 1.3 solution. At M = 1.05, five minutes were required to compute the coarse and medium grids.

6.0 RESULTS FOR FLOW ABOUT A SPHERE

6.1 Program Checks

As a check on the program a mass balance was made to see how the mass flow across the circle of radius HK (Fig. 1) compared with that across AB. Table 4 shows the total mass inflow together with the mass outflow. Good agreement is noted.

As a further check comparisons were made with the results of South's axisymmetric program RAXBOD (Ref. 2) which treats the whole flow field extending to infinity and does not allow for discrete shocks jumps; 'shocks' appear as discontinuities in the velocity components. Results of the comparisons are shown in Figures 4 and 5. These show Mach number distributions along the body and also along the axis of symmetry for free stream Mach numbers 1.3 and 1.02. The M = 1.02 results have not converged to the preset accuracy requirement. However it can be seen that agreement is good when fine meshes are used with the exception of Mach number behaviour in the supersonic zone along the body. Here first order accuracy is used so that a larger discrepancy is expected and also the cutoff line (not used in RAXBOD) may have an effect on the SHOCKFIT results.

6.2 Residuals

At the end of each computation one extra pass is made to calculate residuals at each point (with ϕ_{St} factor α set to zero). The size of the residual does not mean too much unless we compare it with a relevant quantity. Here we compare residuals with the right hand side (d) of the equation

$$a\phi^{+}_{i\,j-1} + b\phi^{+}_{i\,j} + c\phi^{+}_{i\,j+1} = d$$

which is the finite difference form of the equation of motion. The residuals and right hand sides are printed in Tables 5 and 6 for Mach numbers 1.3 and 1.02 (the latter at the fine mesh have not converged). Note that the residuals at the line next to the shock are much smaller at M = 1.02 than at M = 1.3. This is probably due to the entropy change across the shock being much bigger at the larger Mach number and this change is inconsistent with the isentropic assumption for the rest of the flow field.

6.3 Shock Wave Location

The main results of the paper are given in Table 7 which shows the distance F (θ) of the shock wave from the co-ordinate origin for polar angles θ of 0, 18, 36, 54, 72 and 90°. It can be seen that results depend quite strongly on mesh size. The main problem is to be sure of accuracy at θ = 0° since it is here that the correlation with experimental results will be made.

First let us see how much accuracy is needed in F (0) so that the free stream Mach number can be determined to an accuracy ΔM. To do this we need to know an approximate relation between F (0) and M. Such a relation is given in NACA 2000 (Ref. 8) i.e.

$$F(0) = \frac{4}{3}(M-1)^{-1/3} + 0.5$$

(see Fig. 6 to compare this form with the numerical computations). A change of less than ΔM in M thus requires

$$\Delta F(0) < \frac{4}{9}(M-1)^{-4/3}\ \Delta M\ .$$

Taking $\Delta M = 0.002$ we can deduce limiting values for $\Delta F(0)$ as shown in Table 8. The last column in the table shows the limiting value for $\Delta \ln (F(0) - 0.5)$ and can be calculated as

$$\Delta \ln (F(0) - 0.5) = -\frac{1}{3}\ \frac{\Delta M}{M-1}\ .$$

The size of this latter quantity is marked by a symbol I on Figure 6 which shows $\ln (F(0) - 0.5)$ versus $-\ln (M-1)$.

Now observing Table 7 we see that the 5 X 10 and 10 X 20 results for stand-off distance ($\equiv F(0) - 1.5$) differ by quite a large amount so that an extrapolated zero mesh size solution should be used. This latter solution is obtained by extrapolating the 5 X 10 and 10 X 20 solutions by assuming the error is of order mesh size squared — the resulting values are given in Table 7 by the name EXT1. It can be noted that at M = 1.3 the EXT1 result is practically identical to that obtained by carrying out a similar extrapolation from the 10 X 20 and 20 X 40 grids (called EXT2 in Table 7). At M = 1.06 the difference in F (0) between the EXT1 and EXT2 results is 0.01 — well within the accuracy requirement given in Table 8. Thus we can have some confidence in the accuracy of extrapolation from the 5 X 10 and 10 X 20 results and so we propose that the EXT1 results are our final results with accuracy sufficient to be used to correlate stand-off distance to Mach number. We use this procedure rather than compute further solutions on the 20 X 40 grid since computation is rather expensive on the fine grid ($88 at M = 1.06).

Using the EXT1 results we note that, on the log scales of Figure 6, they lie almost on a straight line given by

$$\ln (F(0) - 0.5) = -0.505\ \ln (M-1) - 0.045$$

or

$$F(0) = 0.5 + 0.956\ (M-1)^{-0.505} \qquad (27)$$

The values given by this formula are also tabulated in Table 7. Notice that the differences between F (0) given by (27) and F (0) given by EXT1, for $M \leq 1.08$, are much less than the acceptable tolerances given in Table 8 — given some confidence in our straight line fit.

The RAXBOD results for stand-off distance, given in Figure 6, are found by interpolating between Mach numbers calculated along the axis of symmetry to find at what distance from the body the Rankine Hugoniot value of Mach number is realized. This procedure should give reasonable accuracy since Mach numbers calculated at some distance from the calculated shock discontinuity are considered accurate and the discontinuity, from experience, is always upstream of the real shock jump. Plots of M(axis) from RAXBOD are shown in Figures 4b and 5b.

In the work of Frank and Zeirep (Ref. 11), who use a modification of a formula derived for slender bodies, is given the formula

$$F(0) - 0.5 = 2\left(\frac{0.14\ (\gamma+1)\ M^2}{M^2 - 1}\right)^{2/3}$$

Values obtained by this formula are plotted on Figure 6. It can be seen that the slope of this curve is significantly greater than the slope of our curve thus predicting much larger stand-off distances when $M < 1.10$. Hopefully experiments at these low Mach numbers, to be performed shortly at NAE, will settle the discrepancy.

The shock shapes are compared with experimental data from NACA 2000 (Ref. 8) in Figure 7. It can be seen that satisfactory agreement is obtained.

7.0 CONCLUSIONS

We have used Jameson's rotated difference scheme combined with a Newton iteration of the shock wave to obtain a prediction of the shock wave stand-off distance from a sphere. The same method could also be applied to more general axisymmetric bodies.

As far as is known this is the only rigorous theoretical work which predicts the flow field solution and shock wave location for Mach numbers less than 1.05. Frank and Zeirep in their prediction use a semi-empirical formula based on a modification of slender body theory while Hsieh, using the time dependent approach, takes more than 22 hours for a (nonconverged) solution at $M = 1.05$. The present method needs about five minutes at this Mach number.

The accuracy of the present method can be seen to be fairly good at Mach numbers 1.62, 1.3 and 1.17 at which results have been compared with experiment. Experiments to be performed shortly at NAE at the lower Mach numbers will be used for a further comparison.

Our results (referring to stand-off distance) of best accuracy, given by extrapolating to zero mesh size from a 5×10 and a 10×20 grid, lie practically on a straight line when plotted on the log scales of Figure 6. The resulting formula for $F(0)$ is given by (27).

8.0 REFERENCES

1. Jameson, A. — *Iterative Solution of Transonic Flows Over Airfoils and Wings, Including Flows at Mach 1.* Comm. Pure Appl. Math., Vol. XXVII, 1974, pp. 283-309.

2. South, J.C., Jr.; Jameson, A. — *Relaxation Solutions for Inviscid Axisymmetric Transonic Flow Over Blunt or Pointed Bodies.* Proc. AIAA Comp. Fluid Dynamics Conf., July 1973, pp. 8-17.

3. Barnwell, R.W.; Davis, R.M. — *A Computer Program for Calculating Inviscid Adiabatic Flow About Blunt Bodies Travelling at Supersonic and Hypersonic Speeds at Angle of Attack.* NASA TM X-2334, September 1971.

4. Belotserkovskiy, O.M. — *Supersonic Gas Flow Around Blunt Bodies.* NASA TT F-453, June 1967.

5. Jones, D.J.; South, J.C., Jr.; Klunker, E.B. — *On the Numerical Solution of Elliptic Partial Differential Equations by the Method of Lines.* J. Comp. Phys., 9, 1972, pp. 496-527.

6. Jurak, K.; Pert, G.J.; Capjack, C.E. — *Least Squares Solution for the Blunt Body Hypersonic Flow Problem.* J. Comp. Phys., 10, 1972, pp. 369-373.

7. Harris, H. — NASA Langley. Private Communication.

8 Heberle, J.W., Wood, G.P., Gooderum, P.B. — *Data on Shape and Location of Detached Shock Waves on Cones and Spheres.* NACA TN-2000, January 1950.

9. Aungier, R.H. — *A Computational Method for Exact, Direct and Unified Solutions for Axisymmetric Flow Over Blunt Bodies of Arbitrary Shape.* (Program Blunt) AFWL-TR-70-16, July 1970.

10. Hsieh, T. — *Flow Field Study About a Hemispherical Cylinder in Transonic and Low Supersonic Mach Number Range.* AIAA Paper , January 1975, pp. 75-83.

11. Frank, W., Zeirep, J. — *Transonic Supersonic Flow Around Bodies of Revolution.* Acta Mechanica, 19, 1974, pp. 277-287.

9.0 ACKNOWLEDGEMENTS

Many thanks are due, from the first author, to Bud Bobbitt and Jerry South of NASA Langley for allowing him to pursue this research while on leave at NASA Langley. Thanks also to the rest of the High Speed Aerodynamics Section at Langley for their help and encouragement with Venture 22.

TABLE 1

VALUES OF S_2 AND A_0 DURING THE ITERATION PROCESS M = 1.02

ITN #	5 X 10 Mesh		10 X 20 Mesh		20 X 40 Mesh	
	S_2	A_0*	S_2	A_0	S_2	A_0
0	1.6, -7	6.553	3.6, -3	6.666	1.3, -3	6.941
5	3.6, -6		2.0, -2		1.8, -3	
10	4.6, -7		1.1, -3		2.1, -4	
15	1.2, -6		3.4, -4		7.3, -5	6.995
20	8.8, -7		1.0, -4		7.7, -5	
25	4.9, -7		4.5, -5		8.6, -6	7.017
30	2.5, -7		2.4, -5		2.9, -5	
35	1.3, -5	6.532	1.3, -5	6.722	1.0, -5	
40	3.3, -6		3.4, -5		1.0, -5	7.029
45	1.1, -6		3.7, -6	6.747	1.1, -5	
50	5.2, -7		9.1, -6		Iteration terminated	
55	2.6, -7		1.1, -5	6.791		
60	1.3, -7	6.582	1.5, -5			
65	3.3, -6		1.6, -5	6.841		
70	2.8, -7		1.8, -5			
75	2.0, -6	6.632	1.6, -5	6.891		
80	9.2, -7		1.7, -5			
85	1.6, -6	6.661	1.6, -5	6.941		
90	2.4, -7		1.7, -5			
95	6.2, -8	6.666	Iteration terminated			
100	3.3, -8					

* Shock wave coefficients were changed during the five iterations previous to the listed value.

TABLE 2

VALUES OF $\Sigma\Delta\phi_{i\,j}^2$ AND A_0 DURING THE ITERATION PROCESS M = 1.3

ITN #	5 X 10 Mesh		10 X 20 Mesh		20 X 40 Mesh	
	S_2	A_0*	S_2	A_0	S_2	A_0
0	2.3, -1	2.5	1.9, -3	2.397	4.4, -4	2.414
5	1.7, -1		9.4, -5		7.6, -5	2.416
10	3.4, -2		9.3, -5	2.408	1.1, -5	2.419
15	5.5, -4		8.6, -6	2.411	6.2, -6	
20	2.6, -5		5.8, -6	2.413	2.1, -6	
25	6.3, -4	2.450	2.2, -6		1.3, -6	
30	3.5, -6	2.411	2.0, -6	2.414	6.3, -7	
35	8.3, -6		1.8, -7		3.6, -7	
40	1.5, -5	2.402				
45	2.1, -6	2.398				
50	2.2, -7	2.397				
55	2.5, -8					

* Shock wave coefficients were changed during the five iterations previous to the listed value.

TABLE 3

PROGRESS OF ITERATIONS M = 1.3, 5 X 10 MESH, $\phi_{i\,j}$ = 0 INITIALLY

Shock Change Made on ITN #			Shock Coefficients					
	S_2	S_1	A_0	A_i	A_2	A_3	A_4	A_5
0	2.3, -1		2.5	-0.1	0	0	0	0
24	4.6, -6	1.0, -2	2.450	-0.1184	0.0514	-0.0270	0.0082	-0.0010
30	3.5, -6	1.3, -3	2.411	-0.1251	0.0773	-0.0370	0.0122	-0.0018
37	2.8, -6	2.0, -4	2.402	-0.1235	0.0785	-0.0377	0.0138	-0.0021
42	1.8, -6	9.9, -5	2.398	-0.1242	0.0810	-0.0394	0.0145	-0.0021
46	9.2, -7	7.9, -5	2.397	-0.1242	0.0811	-0.0391	0.0142	-0.0020
55	2.5, -8		No Further Change					

TABLE 4

CHECK ON MASS CONSERVATION

M	Mesh	Mass Flow	
		Across HK	Across AB
1.62	5 X 10	7.90	8.04
1.3	5 X 10	23.10	23.09
	10 X 20	23.24	23.26
	20 X 40	23.28	23.31
1.7	5 X 10	56.74	56.71
	10 X 20	57.93	57.93
1.10	5 X 10	136.3	136.2
	10 X 20	144.7	144.7
1.06	5 X 10	335.1	334.9
	10 X 20	345.3	345.2
1.04	5 X 10	710.9	710.7
	10 X 20	597.1	696.9
1.02	5 X 10	2774	2773
	10 X 20	2659	2659
	20 X 40	2660	2659 (not converged)

TABLE 5a

RESIDUALS AND RIGHT HAND SIDE OF FINITE DIFFERENCE EQUATIONS

AFTER ITERATIONS COMPLETED M = 1.3, 5 × 10 MESH

Line #		(Body) J = 2	3	4	5	6	7	8	9	10	(Line Next to Shock) 11
2	RES	-2.1, -6*	-2.1, -6	-2.3, -6	-2.5, -6	-2.4, -6	-2.3, -6	-2.2, -6	-2.5, -6	-2.9, -6	-2.5, -3
	RHS	7.9, 1	1.0, 1	9.4	6.7	4.4	2.8	1.6	7.8, -1	2.0	-2.7, -1
3		-2.4, -6	-2.3, -7	-3.9, -7	-5.2, -7	-5.3, -7	-4.9, -7	-5.2, -7	-7.7, -7	-1.3, -6	1.7, -3
		6.2, 1	6.2	5.8	4.0	2.4	1.4	7.3, -1	2.7, -1	1.5	-3.1, -1
4		-1.2, -6	-1.3, -6	-1.1, -6	-1.3, -6	-1.6, -6	-1.7, -6	-1.7, -6	-1.9, -6	-1.8, -6	8.9, -4
		3.2, 1	3.4	3.5	2.6	1.7	1.1	5.8, -1	2.4, -1	9.7, -1	-1.8, -1
5		4.2, -5	1.3, -5	1.6, -5	1.2, -5	6.8, -6	-4.8, -8	-5.6, -8	-2.4, -6	-7.3, -6	3.1, -5
		8.4	2.4	1.8	1.1	6.4, -1	3.9, -1	2.4, -1	1.0, -1	5.0, -1	-9.7, -2
6		1.4, -4	4.5, -5	7.4, -5	1.0, -4	1.1, -4	1.0, -4	9.1, -5	9.2, -5	9.3, -5	-2.8, -3
		-3.7	2.0	1.1	5.8, -1	2.9, -1	1.2, -1	4.1, -2	-2.3, -3	2.3, -1	-5.1, -2
7		6.3, -5	-9.7, -5	-2.5, -4	-2.7, -4	-2.9, -4	-3.6, -4	-5.0, -4	-6.7, -4	-5.7, -4	-9.4, -3
		-6.3	1.7	5.2, -1	2.5, -1	1.2, -1	5.0, -2	1.3, -2	-6.6, -3	1.2, -1	-1.5, -2

* -2.1, -6 is equivalent to -2.1×10^{-6}

TABLE 5b

RESIDUALS AND RIGHT HAND SIDES OF FINITE DIFFERENCE EQUATIONS

AFTER ITERATIONS COMPLETED M = 1.3, 20 × 40 MESH

Line #		(Body) J = 2	6	10	14	18	22	26	30	34	38	(Line Next to Shock) 41
2	RES	-3.9, -4	-3.7, -4	-3.5, -4	-3.2, -4	-2.9, -4	-2.5, -4	-2.1, -4	-1.8, -4	-1.5, -4	-1.1, -4	-1.5, -2
	RHS	4.0, 2	1.0, 2	9.1, 1	7.4, 1	5.7, 1	4.1, 1	2.8, 1	1.7, 1	8.7	3.1	8.6, -2
6		-4.1, -4	-6.1, -5	-5.8, -5	-5.3, -5	-4.7, -5	-4.1, -5	-3.5, -5	-3.2, -5	-3.6, -5	-4.9, -5	-1.2, -2
		2.8, 2	4.6, 1	4.2, 1	3.4, 1	2.6, 1	1.9, 1	1.3, 1	7.6	3.9	1.2	-2.1, -1
10		-1.1, -3	-9.1, -5	-8.9, -5	-8.4, -5	-7.8, -5	-7.3, -5	-6.9, -5	-6.7, -5	-6.9, -5	-7.3, -5	-1.2, -2
		1.3, 2	1.7, 1	2.1, 1	2.0, 1	1.8, 1	1.4, 1	9.3	5.6	2.8	8.7, -1	-1.2, -1
14		-2.4, -3	-3.5, -4	-2.4, -4	-1.6, -4	-1.1, -4	-9.3, -5	-8.7, -5	-9.2, -5	-1.1, -4	-1.5, -4	-6.4, -3
		3.6, 1	1.0, 1	7.1	4.9	3.5	4.2	3.6	2.5	1.1	3.2, -1	-9.5, -2
18		-5.9, -3	-1.5, -3	-1.1, -3	-8.9, -4	-7.3, -4	-5.6, -4	-3.5, -4	-2.0, -4	-2.1, -4	-2.9, -4	-1.6, -2
		-1.6, 1	9.2	3.9	1.7	7.7, -1	4.0, -1	2.3, -1	1.2, -1	3.8, -2	-3.3, -2	-8.7, -2
22		-1.6, -2	-5.6, -3	-3.8, -3	-2.8, -3	-2.2, -3	-2.0, -3	-1.9, -3	-1.8, -3	-1.7, -3	-1.5, -3	-3.7, -2
		-2.9, 1	3.9	6.6, -1	3.3, -1	2.5, -1	1.5, -1	6.4, -2	1.7, -2	-1.1, -2	-3.7, -2	-3.8, -2

TABLE 6a

RESIDUALS AND RIGHT HAND SIDES OF FINITE DIFFERENCE EQUATIONS

AFTER ITERATIONS COMPLETED M = 1.02, 5 X 10 MESH

Line #		(Body) J = 2	3	4	5	6	7	8	9	10	(Line Next to Shock) 11
2	RES	-1.4,-4	-5.8,-4	-2.2,-4	-9.6,-5	-4.4,-5	-1.9,-6	3.2,-5	3.1,-5	8.2,-6	1.2,-6
	RHS	1.4, 2	2.6, 1	8.3	4.1	2.0	9.4,-1	4.1,-1	1.7,-1	6.7,-2	1.8,-2
3		5.8,-5	-2.7,-4	-3.0,-5	1.3,-5	1.6,-6	-6.3,-6	6.1,-6	1.7,-5	5.4,-6	1.1,-6
		1.1, 2	2.0, 1	4.8	2.0	9.4,-1	4.2,-1	1.8,-1	7.1,-2	2.9,-2	6.9,-3
4		1.1,-4	-1.5,-4	-1.8,-5	7.6,-6	2.4,-6	-2.1,-7	8.0,-6	1.8,-5	4.3,-6	1.0,-6
		6.3, 1	1.2, 1	3.5	1.6	7.3,-1	3.0,-1	1.2,-1	4.3,-2	1.8,-2	3.5,-3
5		1.2,-4	-4.6,-5	7.1,-6	6.9,-6	7.9,-7	4.2,-6	1.3,-5	2.2,-5	1.1,-6	1.6,-6
		1.2, 1	4.3	1.2	8.2,-1	3.6,-1	1.3,-1	4.5,-2	1.5,-2	6.8,-3	6.3,-4
6		2.3,-4	4.2,-5	-1.9,-5	-1.9,-5	-6.0,-6	9.9,-6	2.6,-5	3.2,-5	-6.6,-6	-1.9,-6
		-1.1, 1	8.5,-1	4.0,-1	7.7,-2	5.9,-2	1.9,-2	5.0,-3	1.2,-3	1.4,-3	-3.1,-4
7		-3.3,-4	3.4,-4	5.2,-5	9.4,-6	1.6,-5	3.4,-5	3.2,-5	2.1,-5	3.8,-6	-7.5,-7
		-6.6	3.7,-1	1.8,-2	2.7,-4	-9.5,-4	-4.9,-4	-2.2,-4	-1.2,-4	1.4,-4	-7.3,-5

TABLE 6b

RESIDUALS AND RIGHT HAND SIDES OF FINITE DIFFERENCE EQUATIONS

AFTER ITERATIONS COMPLETED M = 1.02, 20 X 40 MESH (NOT CONVERGED)

Line #		(Body) J = 2	6	10	14	18	22	26	30	34	38	(Line Next to Shock) 41
2	RES	-3.1,-2	-3.0,-2	-2.6,-2	-2.0,-2	-1.1,-2	-3.7,-3	-2.4,-3	-9.6,-4	5.0,-4	1.4,-4	-2.2,-5
	RHS	6.6, 2	1.8, 2	1.2, 2	7.6, 1	3.9, 1	1.7, 1	7.1	2.8	1.0	3.0,-1	5.1,-2
6		-2.3,-2	-6.7,-4	-6.4,-4	-4.9,-4	-5.3,-4	-2.9,-4	-2.7,-4	-5.8,-4	9.3,-5	9.7,-5	2.0,-6
		4.9, 2	8.4, 1	5.7, 1	3.6, 1	1.8, 1	7.8	3.2	1.2	4.4,-1	1.3,-1	2.1,-2
10		-3.6,-2	-1.9,-4	-4.0,-4	-4.1,-4	-3.7,-4	-1.9,-4	-2.4,-4	-5.2,-4	6.5,-5	6.1,-5	-2.1,-5
		2.4, 2	3.8, 1	3.6, 1	2.6, 1	1.3, 1	5.5	2.1	7.5,-1	2.6,-1	7.3,-2	1.1,-2
14		-4.0,-2	2.5,-4	1.0,-4	-2.4,-4	-3.2,-4	-1.3,-4	-2.3,-4	-3.9,-4	5.2,-5	-1.1,-5	2.1,-6
		3.8, 1	1.5, 1	8.0	1.1, 1	6.4	2.4	8.1,-1	2.7,-1	8.7,-2	2.3,-2	3.0,-3
18		-3.3,-2	-4.8,-5	-7.7,-5	-8.5,-5	-2.0,-5	-2.6,-4	-4.4,-4	-1.7,-4	-7.6,-6	-3.4,-5	-2.3,-5
		-5.7, 1	1.2, 1	2.5	7.2,-1	1.2	3.9,-1	1.1,-1	3.2,-2	9.3,-3	2.0,-3	-3.9,-5
22		-1.4,-2	-1.2,-3	-1.1,-3	-2.7,-4	1.7,-4	-2.7,-4	-1.0,-4	-7.3,-5	-5.5,-5	-2.7,-6	-7.5,-5
		-2.4, 1	7.9,-1	8.0,-2	1.3,-3	2.2,-2	3.9,-3	5.5,-4	-2.2,-6	-7.7,-5	-8.7,-5	-7.0,-5

TABLE 7

DISTANCE OF SHOCK FROM ORIGIN FOR DIFFERENT θ VALUES, i.e. F(θ). EXT1, EXT2 = VALUES EXTRAPOLATED FROM 5 × 10, 10 × 20 AND 10 × 20, 20 × 40 GRIDS

M	NSH	Mesh	$\theta = 0$	18	36	54	72	90	F(0) by Formula (27)
1.62	6	5 × 10	2.002	2.032	2.145	2.391	2.866	3.823	
1.3	6	5 × 10	2.397	2.459	2.670	3.115	4.007	5.998	
	6	10 × 20	2.414	2.476	2.686	3.131	4.028	6.016	
	6	20 × 40	2.419	2.481	2.692	3.137	4.037	6.020	
	6	EXT1	2.420	2.482	2.691	3.134	4.035	6.022	
	6	EXT2	2.421	2.483	2.693	3.139	4.040	6.021	
1.17	6	5 × 10	2.865	2.962	3.287	3.980	5.452	9.203	
		10 × 20	2.911	3.008	3.338	4.040	5.530	9.300	
		EXT1	2.926	3.023	3.355	4.060	5.556	9.332	
1.10	6	5 × 10	3.455	3.592	4.057	5.075	7.369	14.165	3.558
		10 × 20	3.554	3.694	4.172	5.218	7.577	14.594	
		EXT1	3.587	3.728	4.210	5.266	7.646	14.737	
1.08	6	5 × 10	3.756	3.913	4.447	5.632	8.381	17.156	3.923
		10 × 20	3.888	4.049	4.601	5.826	8.671	17.774	
		EXT1	3.932	4.094	4.652	5.891	8.768	17.980	
1.06	6	5 × 10	4.202	4.386	5.020	6.452	9.902	22.154	4.458
		10 × 20	4.388	4.580	5.241	6.735	10.337	23.116	
		20 × 40	4.427	4.620	5.286	6.791	10.416	23.240	
		EXT1	4.450	4.645	5.315	6.829	10.482	23.437	
		EXT2	4.440	4.633	5.301	6.810	10.442	23.281	
1.05	6	5 × 10	4.525	4.729	5.435	7.045	11.023	26.199	4.840
		10 × 20	4.750	4.963	5.702	7.388	11.556	27.403	
		EXT1	4.825	5.041	5.791	7.502	11.734	27.804	
1.04	6	5 × 10	4.954	5.184	5.982	7.828	12.529	32.243	5.358
		10 × 20	5.249	5.491	6.334	8.284	13.248	33.843	
		EXT1	5.346	5.592	6.450	8.434	13.483	34.368	
1.03	6	5 × 10	5.568	5.833	6.761	8.942	14.716	42.248	6.117
		10 × 20	5.983	6.267	7.260	9.594	15.757	44.463	
		EXT1	6.121	6.412	7.426	9.811	16.104	45.201	
1.02	6	5 × 10	6.666	6.992	8.145	10.907	18.629	63.661	7.393
		10 × 20	7.227	7.579	8.821	11.794	20.029	65.381	
		EXT1	7.414	7.775	9.046	12.090	20.496	65.954	
1.01									10.283

TABLE 8

REQUIRED ACCURACY IN SHOCK LOCATION
TO GIVE MACH NUMBER ACCURATE TO $\Delta M = 0.002$

M	Accuracy Required in F(0)	Accuracy Required in ln (F(0) - 0.5)
1.3	0.004	0.002
1.10	0.019	0.007
1.08	0.026	0.008
1.06	0.038	0.011
1.05	0.048	0.013
1.04	0.065	0.016
1.03	0.095	0.022
1.02	0.163	0.033
1.01	0.412	0.066

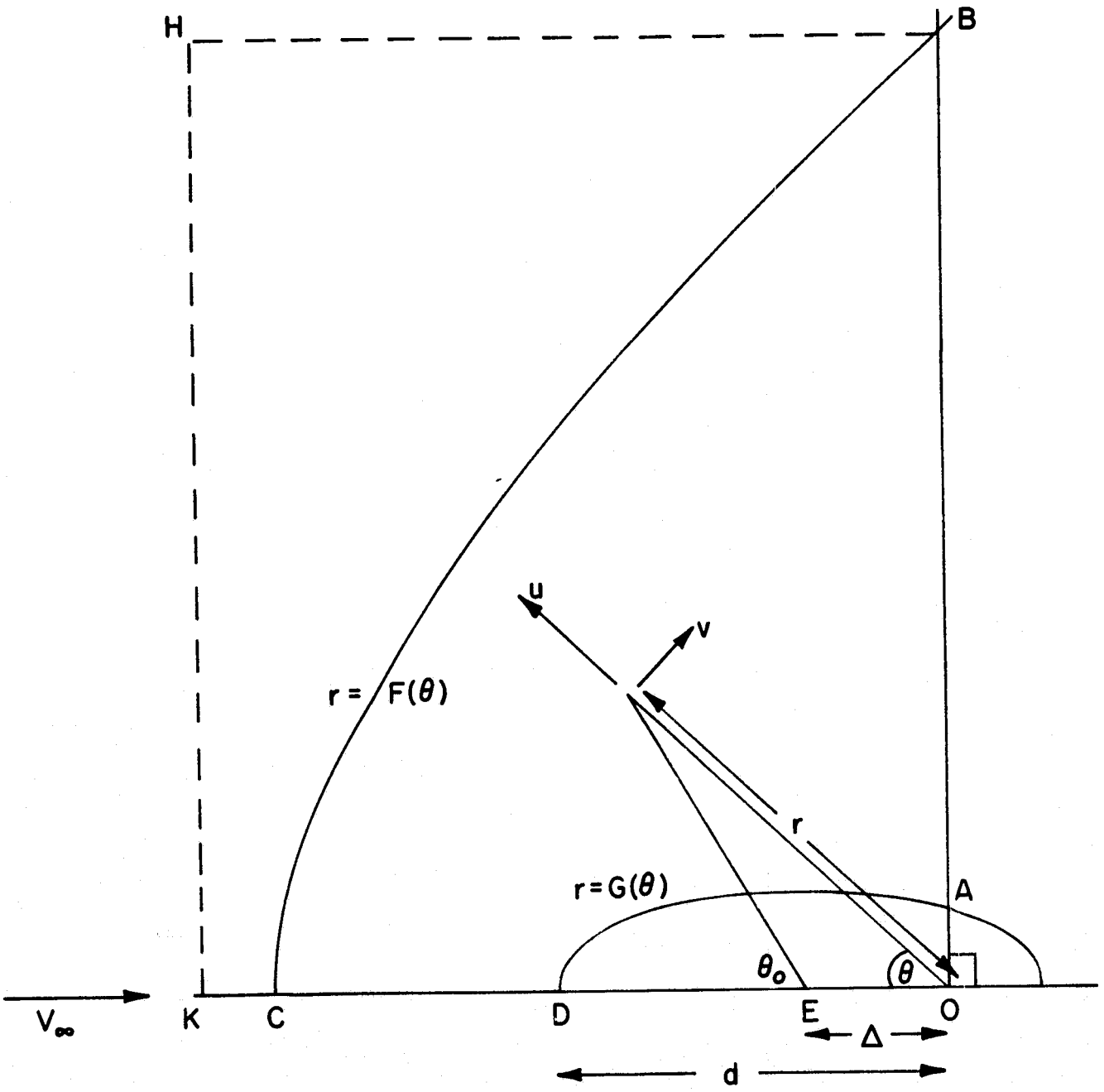

FIG. 1: CO-ORDINATE SYSTEM

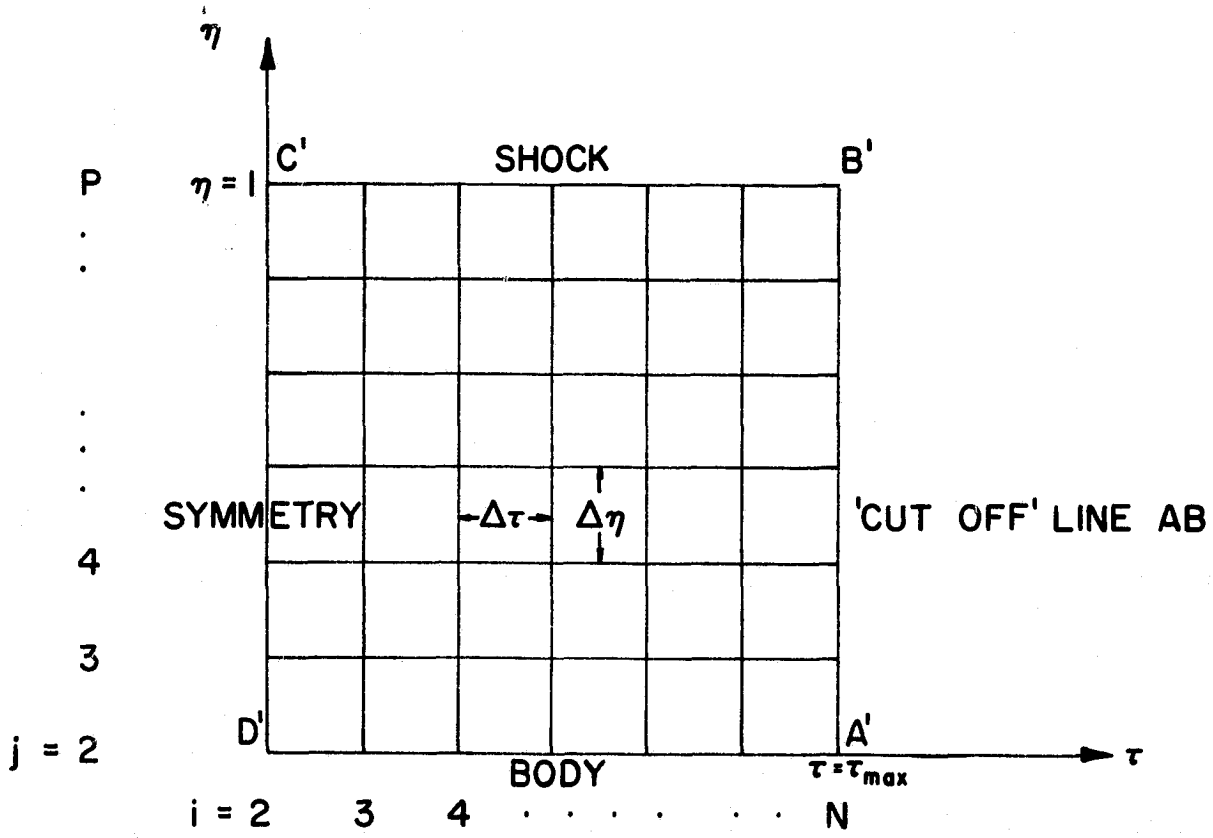

FIG. 2: THE COMPUTATIONAL GRID

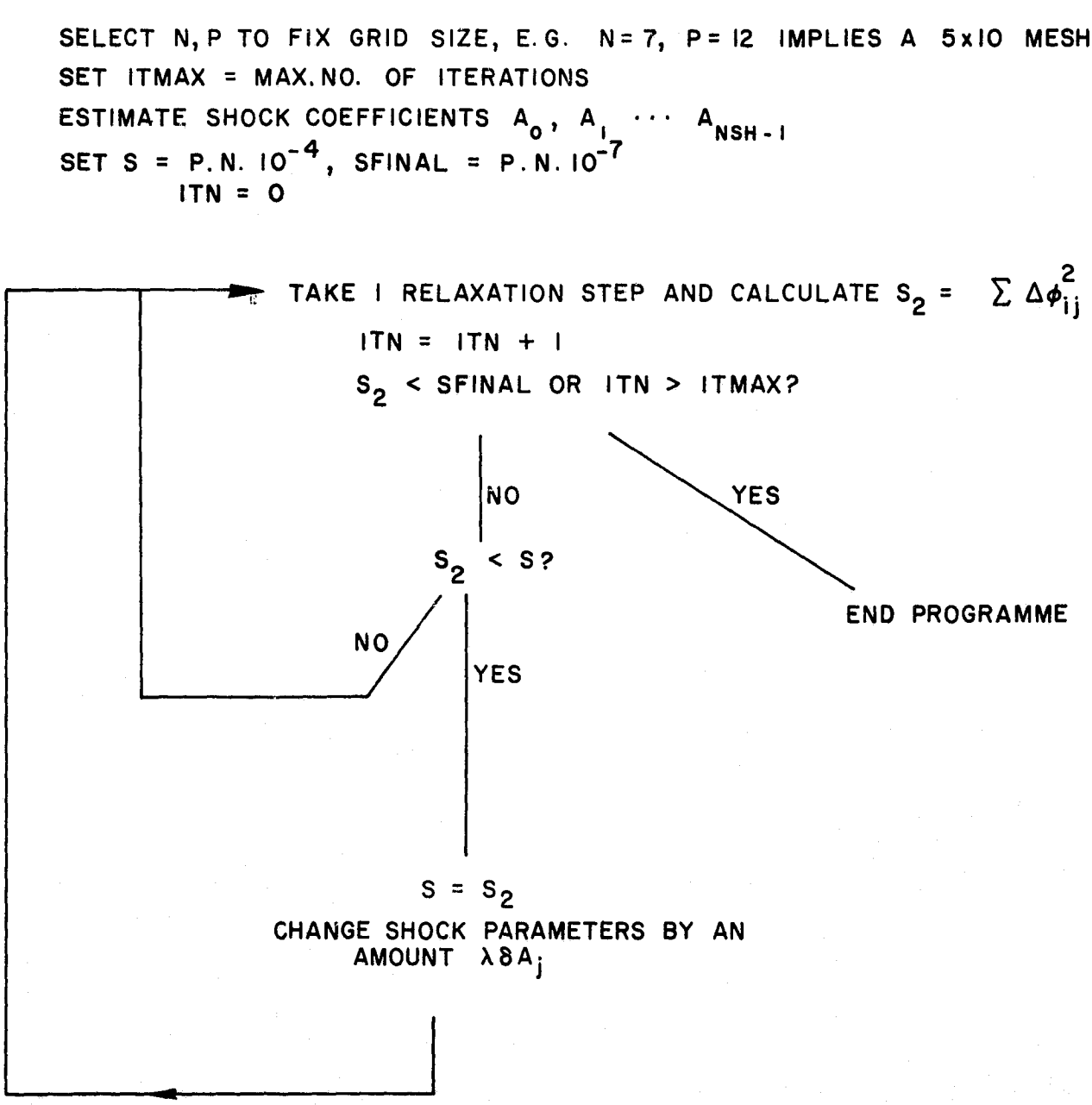

FIG. 3: FLOW DIAGRAM SHOWING THE INNER AND OUTER ITERATION LOOPS

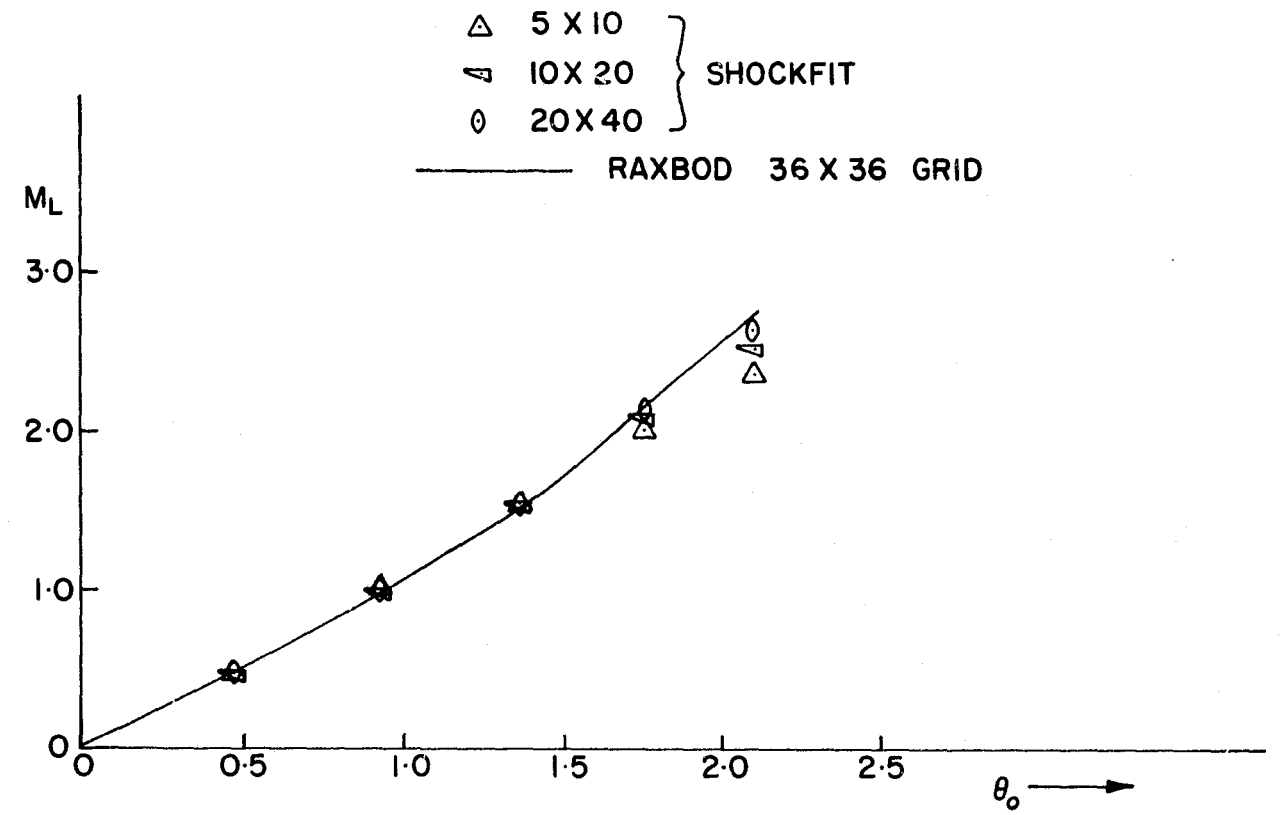

4a. MACH NUMBER VERSUS DISTANCE ALONG SPHERE

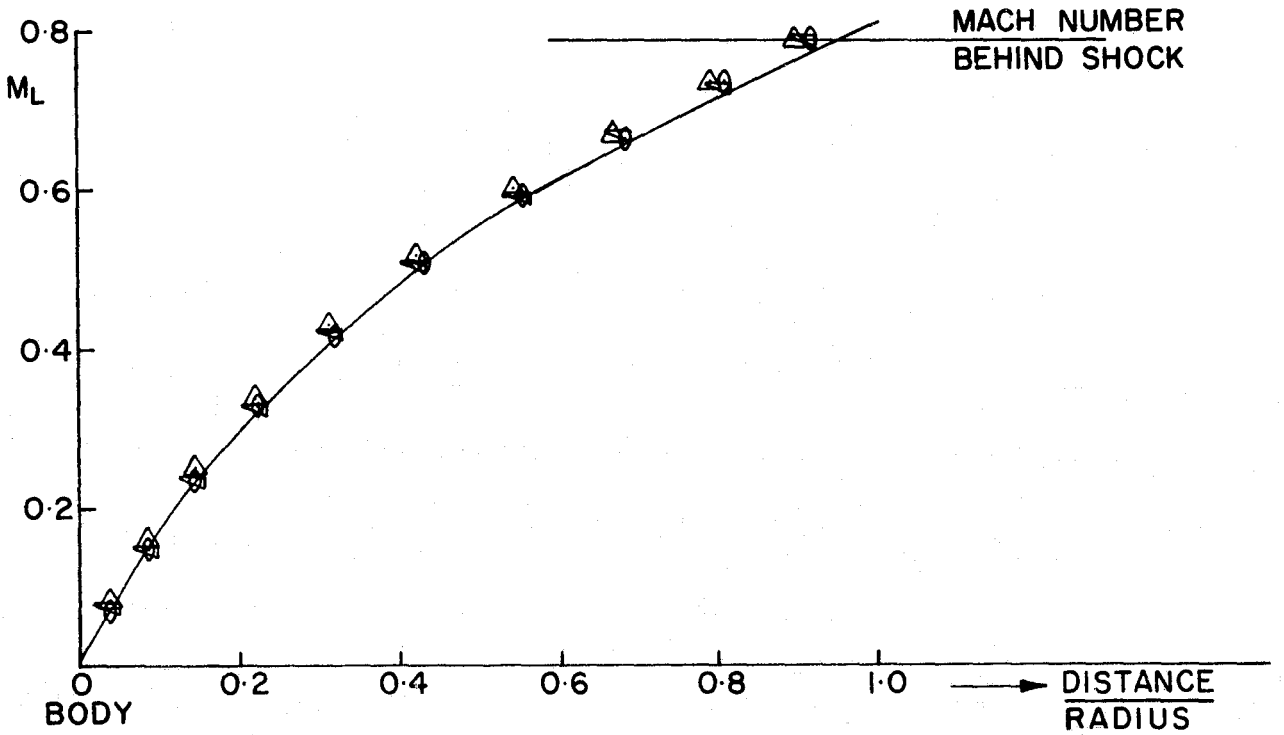

4b. MACH NUMBER VERSUS DISTANCE ALONG AXIS OF SYMMETRY

FIG. 4: RAXBOD COMPARED WITH PRESENT RESULTS, M=1·3

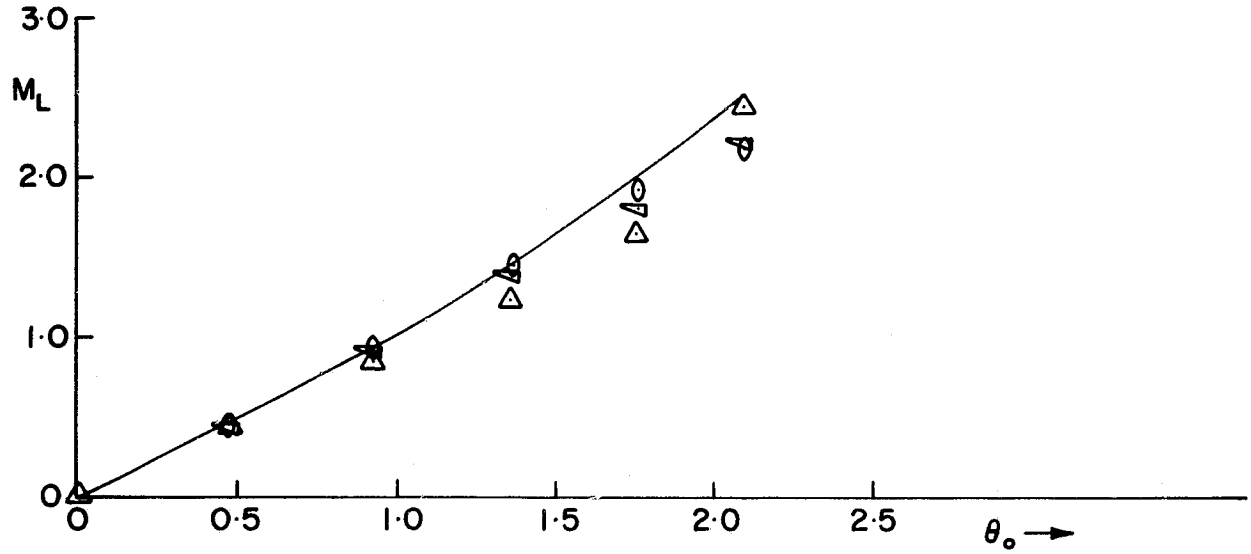

5a. MACH NUMBER VERSUS DISTANCE ALONG SPHERE

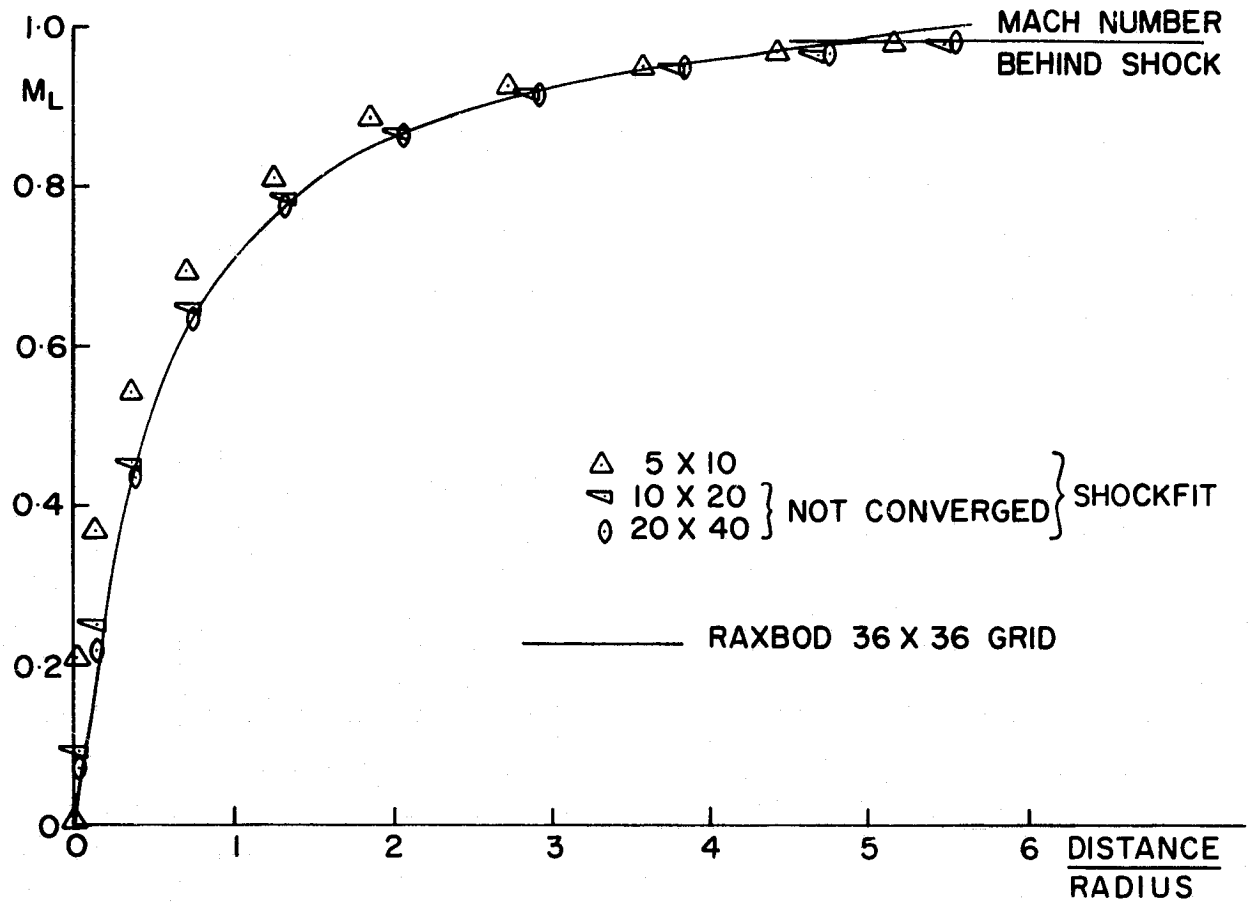

5b. MACH NUMBER VERSUS DISTANCE ALONG AXIS OF SYMMETRY

FIG. 5: RAXBOD COMPARED WITH PRESENT RESULTS, M = 1·02

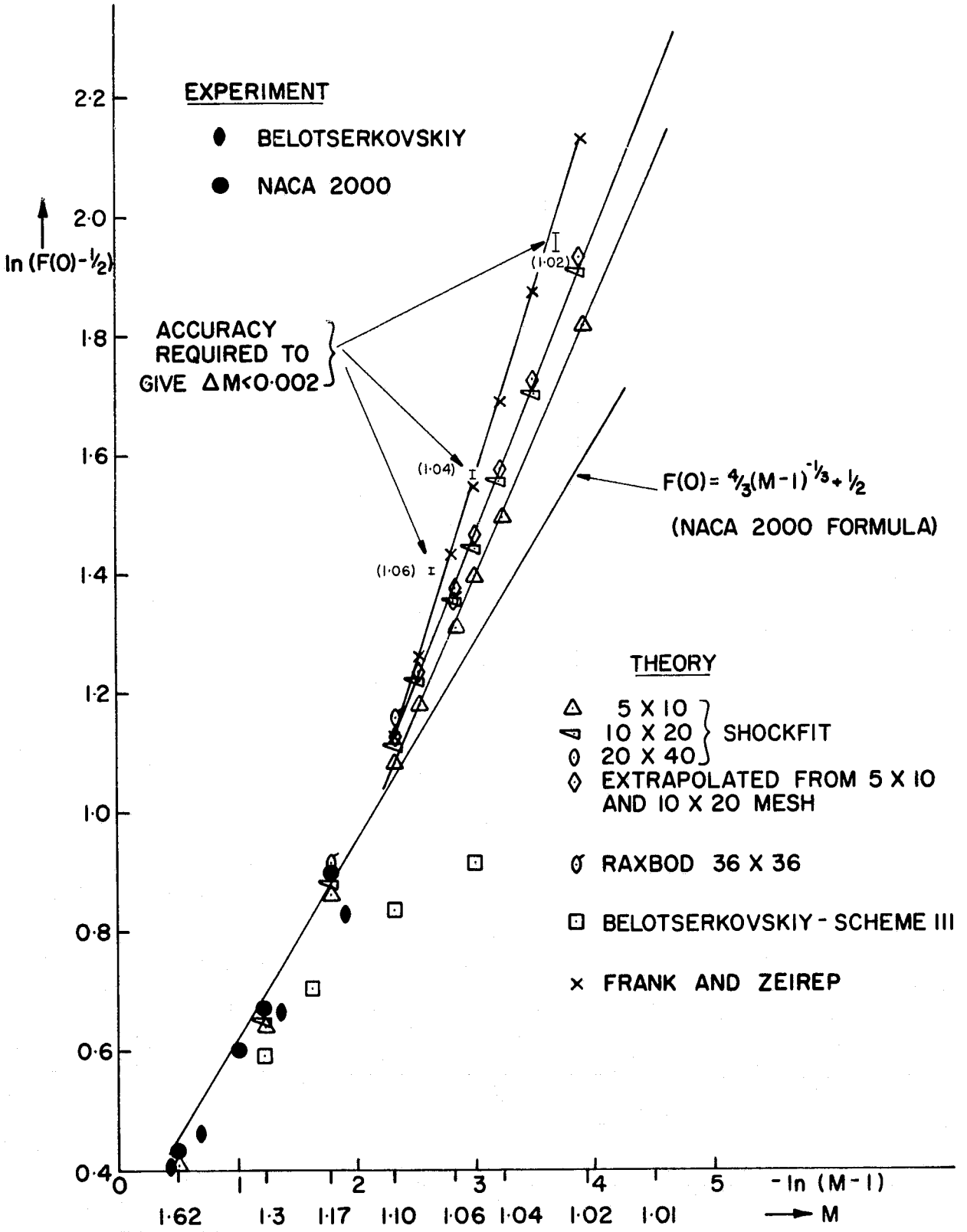

FIG.6: SHOCK WAVE STAND-OFF DISTANCE VERSUS MACH NUMBER

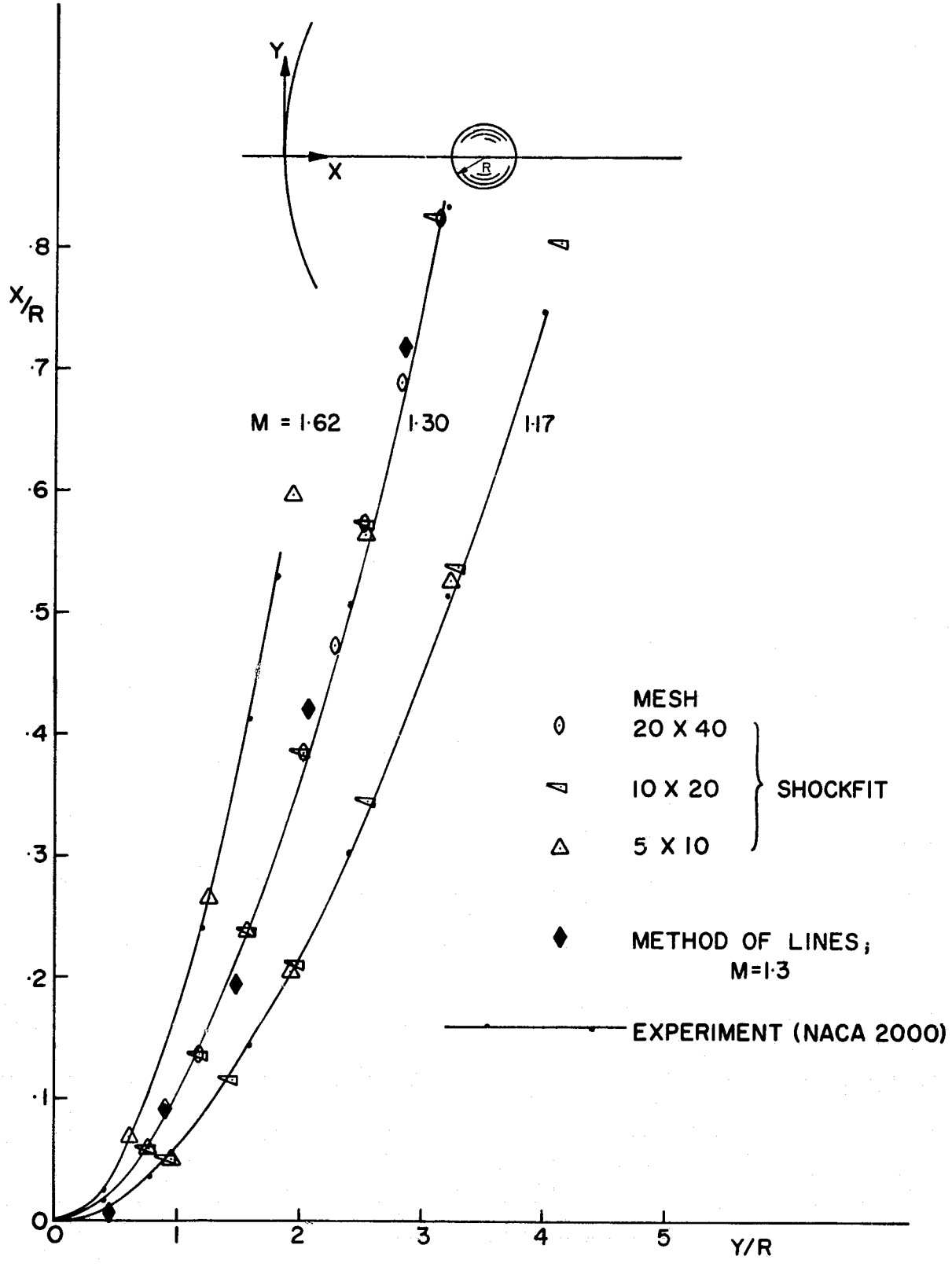

FIG. 7: COMPARISON OF SHOCK SHAPES

APPENDIX A

The $\theta \rightarrow \sigma$ Transformation

Consider part of the transformation (1) i.e.

$$\theta = a\sigma^3 + b\sigma \ .$$

Let

$$\sigma = \sigma_M \text{ at } \theta = \frac{\pi}{2}$$

hence

$$\frac{\pi}{2} = a\sigma_M^3 + b\sigma_M \tag{A1}$$

Now we may require to bunch up θ = const co-ordinate lines near the axis of symmetry $\theta = 0$ (this is done in the case of ellipsoid calculations). To do this let

$$(\theta_\sigma)_{\sigma_M} = \bar{\alpha}(\theta_\sigma)_o$$

where $\bar{\alpha}$ is a constant fixed by the user to bunch lines closer together, thus

$$3a\sigma_M^2 + b = \bar{\alpha}b \tag{A2}$$

We fix b = 0.1 and solve (A1) and (A2) for a and σ_M giving

$$\sigma_M = \frac{3\pi/2}{(2 + \bar{\alpha})\, b} \tag{A3}$$

and

$$a = \frac{(\bar{\alpha} - 1)\, b}{3\sigma_M^2} \tag{A4}$$

APPENDIX B

The $\xi \rightarrow \eta$ Transformation (2)

We require

$$\eta = 1 \quad \text{at} \quad \xi = 1$$

and also, to bunch the co-ordinate lines near the body,

$$\left(\frac{d\xi}{d\eta}\right)_{\xi = 0} = g_1 \left(\frac{d\xi}{d\eta}\right)_{\xi = 1/2}$$

$$\left(\frac{d\xi}{d\eta}\right)_{\xi = 1} = g_2 \left(\frac{d\xi}{d\eta}\right)_{\xi = 1/2}$$

where g_1 and g_2 determine the density of the co-ordinate lines near the body and shock relative to the density in the middle. Since the shock departs rapidly from the body as M approaches unity it was felt that g_1 should accordingly grow smaller with Mach number decreasing while g_2 is fixed at 0.8 so that ξ co-ordinate lines are not too sparse near the shock wave. Thus we choose

$$g_1 = M - 1$$

and

$$g_2 = 0.8$$

Now

$$\xi_\eta = A' + 3B'\eta^2 + 4C'\eta^3$$

and so the equations for A', B', C' are

$$A' + B' + C' = 1$$

$$A' = g_1 \left(A' + 3B'\eta_{1/2}^2 + 4C'\eta_{1/2}^3 \right)$$

$$A' + 3B' + 4C' = g_2 \left(A' + 3B'\eta_{1/2}^2 + 4C'\eta_{1/2}^3 \right) = g_2 \frac{A'}{g_1}$$

where $\eta_{1/2}$ is the value of η at $\xi = 1/2$ hence

$$1/2 = A'\eta_{1/2} + B'\eta_{1/2}^3 + C'\eta_{1/2}^4$$

$\eta_{1/2}$ is found using Newton's method while A', B', C' are found from linear analysis.

APPENDIX C

Velocity Components in the (η, τ) Plane

As defined previously (u, v) are the velocity components in the (r, θ) directions. Now let u' be the velocity along τ = const and v' be the velocity along η = const. Thus u', v' are the velocity components along the mesh lines in the (η, τ) plane and as such indicate which backward finite difference expressions to use in the supersonic region.

To find u', v' we let μ be the angle between the line η = const and the line θ = const. Then

$$u = u' + v' \cos \mu$$

and

$$v = v' \sin \mu$$

Now the line η = const is given by

$$0 = \delta\eta = \eta_\xi \delta\xi = \eta_\xi \left(\xi_r \delta r + \delta_\theta \delta\theta\right)$$

and is therefore given by

$$\frac{\delta r}{\delta \theta} = - \frac{\xi_\theta}{\xi_r}$$

so that

$$\tan \mu = \frac{r\delta\theta}{\delta r} = \frac{-r\xi_r}{\xi_\theta}$$

Thus

$$v' = \frac{v\sqrt{\xi_r^2 + \xi_\theta^2/r}}{\xi_r}$$

and

$$u' = u - v' \cos\mu = u - v \cot\mu = u + v \frac{\xi_\theta}{r\xi_r} = \frac{1}{\xi_r}\left(u\xi_r + \frac{v}{r} \xi_\theta\right)$$

referring to (11) it can be seen that u', v' are related to U, V and in fact have the same sign since η_ξ (by definition) and ξ_r $(= 1/(F - G))$ are positive. Thus U and V are used to determine the direction of flow in the supersonic region.

APPENDIX D

Transformation of the Principal Part to Streamline Co-ordinates (S, N)

Consider

$$\left(1 - \frac{q^2}{a^2}\right)\phi_{SS} + \phi_{NN} = \left(\frac{1}{q^2} - \frac{1}{a^2}\right)\left(U^2\phi_{\eta\eta} + 2UV\phi_{\eta\tau} + V^2\phi_{\tau\tau}\right)$$

$$+ \frac{1}{q^2}\left(\bar{V}^2\phi_{\eta\eta} - 2\bar{U}\bar{V}\phi_{\eta\tau} + \bar{U}^2\phi_{\tau\tau}\right)$$

$$= \left(\frac{U^2 + \bar{V}^2}{q^2} - \frac{U^2}{a^2}\right)\phi_{\eta\eta} + 2\left(\frac{UV - \bar{U}\bar{V}}{q^2} - \frac{UV}{a^2}\right)\phi_{\eta\tau}$$

$$+ \left(\frac{V^2 + \bar{U}^2}{q^2} - \frac{V^2}{a^2}\right)\phi_{\tau\tau}$$

Now

$$U^2 + \bar{V}^2 = \left(u\xi_r + \frac{v}{r}\,\xi_\theta\right)^2 \eta_\xi^2 + \left(v\xi_r - \frac{u}{r}\,\xi_\theta\right)^2 \eta_\xi^2$$

$$= \eta_\xi^2\left((u^2 + v^2)\,\xi_r^2 + \frac{u^2 + v^2}{r^2}\,\xi_\theta^2\right)$$

$$= \eta_\xi^2 q^2\left(\xi_r^2 + \frac{\xi_\theta^2}{r^2}\right)$$

and

$$U^2 = \left(u^2\xi_r^2 + \frac{v^2}{r^2}\,\xi_\theta^2 + 2uv\xi_r\,\frac{\xi_\theta}{r}\right)\eta_\xi^2 .$$

Hence

$$\frac{U^2 + \bar{V}^2}{q^2} - \frac{U^2}{a^2} = \eta_\xi^2\left(\xi_r^2 + \frac{\xi_\theta^2}{r^2} - \frac{u^2}{a^2}\,\xi_r^2 - \frac{v^2}{a^2r^2}\,\xi_\theta^2 - \frac{2uv}{a^2}\,\xi_r\,\frac{\xi_\theta}{r}\right)$$

$$= \eta_\xi^2\left[\xi_r^2\left(1 - \frac{u^2}{a^2}\right) - \frac{2uv}{a^2}\,\xi_r\,\frac{\xi_\theta}{r} + \frac{\xi_\theta^2}{r^2}\left(1 - \frac{v^2}{a^2}\right)\right]$$

$$= A\eta_\xi^2 \qquad \text{(see (16a))}$$

The $2\phi_{\eta\tau}$ coefficient is

$$\left(\frac{UV - \bar{U}\bar{V}}{q^2} - \frac{UV}{a^2}\right) = \frac{\sigma_\theta}{q^2}\left[\left(u\xi_r + \frac{v}{r}\,\xi_\theta\right)\eta_\xi\,\frac{v}{r} - \left(v\xi_r - \frac{u}{r}\,\xi_\theta\right)\eta_\xi\,\frac{u}{r}\right]$$

$$- \left(u\xi_r + \frac{v}{r}\,\xi_\theta\right)\frac{\eta_\xi}{a^2}\,\frac{v}{r}\,\sigma_\theta$$

$$= \frac{\sigma_\theta}{q^2}\left[\frac{v^2}{a^2}\,\xi_\theta\eta_\xi + \frac{u^2}{r^2}\,\xi_\theta\eta_\xi\right] - \eta_\xi\sigma_\theta\left(\frac{uv}{a^2 r}\,\xi_r + \frac{v^2}{a^2 r^2}\,\xi_\theta\right)$$

$$= \sigma_\theta\,\frac{\xi_\theta\eta_\xi}{r^2} - \sigma_\theta\eta_\xi\left(\frac{uv}{a^2 r}\,\xi_r + \frac{v^2}{a^2 r^2}\,\xi_\theta\right)$$

$$= \sigma_\theta\eta_\xi\,\frac{\xi_\theta}{r^2}\left(1 - \frac{v^2}{a^2}\right) - \eta_\xi\,\frac{uv}{a^2 r}\,\xi_r\sigma_\theta$$

$$= \eta_\xi\,\frac{B}{2} \qquad \text{(see (16b))}$$

Finally

$$\frac{V^2 + \bar{U}^2}{q^2} - \frac{V^2}{a^2} = \left[\left(\frac{v^2}{r^2} + \frac{u^2}{r^2}\right)/q^2 - \frac{v^2}{a^2 r^2}\right]\sigma_\theta^2$$

$$= \frac{\sigma_\theta^2}{r^2}\left(1 - \frac{v^2}{a^2}\right) = C \qquad \text{(see (16c))}$$

and so

$$\left(1 - \frac{q^2}{a^2}\right)\phi_{SS} + \phi_{NN} = A\eta_\xi^2\phi_{\eta\eta} + B\eta_\xi\phi_{\eta\tau} + C\phi_{\tau\tau}$$

and formula (17) is recovered.

APPENDIX E

Evaluating the Amplification Factor

The equation of motion with the ϕ_{St} term added is

$$\left(1 - \frac{q^2}{a^2}\right)\phi_{SS} + \phi_{NN} - \alpha\phi_{St} = \text{L.O.T.} \tag{E1}$$

(lower order terms)

where

$$q^2\phi_{SS} = U^2\phi_{\eta\eta} + 2UV\phi_{\eta\tau} + V^2\phi_{\tau\tau} \tag{E2}$$

$$q^2\phi_{NN} = \bar{V}^2\phi_{\eta\eta} - 2\bar{U}\bar{V}\phi_{\eta\tau} + \bar{U}^2\phi_{\tau\tau} \tag{E3}$$

For the difference equations in ϕ_{NN} we use

$$\Delta\eta^2\phi_{\eta\eta} = \phi^+_{i,j+1} - 2\phi^+_{ij} + \phi^+_{ij-1} \tag{E4}$$

$$4\Delta\eta\Delta\tau\phi_{\eta\tau} = \phi^+_{i-1,j-1} - \phi^+_{i-1,j+1} - \phi_{i+1,j-1} + \phi_{i+1,j+1} \tag{E5}$$

$$\Delta\tau^2\phi_{\tau\tau} = \phi^+_{i-1,j} - \phi^+_{ij} - \phi_{ij} + \phi_{i+1,j} \tag{E6}$$

while in ϕ_{SS} we use

$$\Delta\eta^2\phi_{\eta\eta} = \phi_{i,j} - 2\phi_{i,j-1} + \phi_{ij-2} \tag{E7}$$

$$\Delta\eta\Delta\tau\phi_{\eta t} = \phi_{i,j} - \phi_{ij-1} - \phi_{i-1,j} + \phi_{i-1,j-1} \tag{E8}$$

$$\Delta\tau^2\phi_{\tau\tau} = \phi_{i,j} - 2\phi_{i-1,j} + \phi_{i-2,j} \tag{E9}$$

assuming, for the analysis, that $U > 0$ and $V > 0$. ϕ_{St} is represented as

$$\phi_{St} = \frac{U}{q}\phi_{\eta t} + \frac{V}{q}\phi_{\tau t}$$

$$= \frac{U}{q}\left(\frac{\phi^+_{ij} - \phi^+_{ij-1} - \phi_{ij} + \phi_{ij-1}}{\Delta\eta\Delta t}\right)$$

$$+ \frac{V}{q}\left(\frac{\phi^+_{ij} - \phi^+_{i-1,j} - \phi_{ij} + \phi_{i-1,j}}{\Delta\tau\Delta t}\right)$$

In order to analyse the convergence of the iteration scheme the above equations have to be simplified. This is done by assuming that $U = \bar{U}$, $V = \bar{V}$ and $U^2 + V^2 = q^2$. An insight into this simpler case may lead to convergence in the more general case.

Let
$$\phi_{i\,j} = G^k e^{im\eta} e^{in\tau} \tag{E10}$$

where G is the amplification factor given by

$$\phi^+_{i\,j} = G\phi_{i\,j}$$

A convergent scheme requires $|G| < 1$. Now let

$$\mu = m\Delta\eta \qquad \text{and} \qquad \upsilon = n\Delta\tau \tag{E11}$$

and substitute the forms (E10), (E11) into (E4) - (E9) and substitute those into (E1) to give

$$\left(1 - M_L^2\right)\left\{\left(1 - 2e^{-i\mu} + e^{-2i\mu}\right)\frac{U^2}{\Delta\eta^2} + \left(1 - e^{-i\mu} - e^{-i\upsilon} + e^{-i\mu}\,e^{-i\upsilon}\right)\frac{2UV}{\Delta\eta\Delta\tau}\right.$$

$$\left. + \left(1 - 2e^{-i\upsilon} + e^{-2i\upsilon}\right)\frac{V^2}{\Delta\tau^2}\right\}$$

$$+ \left\{\left(e^{i\mu} - 2 + e^{-i\mu}\right)\frac{GV^2}{\Delta\eta^2}\right.$$

$$- \left(Ge^{-i(\mu+\upsilon)} - Ge^{-i(\upsilon-\mu)} - e^{i(\upsilon-\mu)} + e^{i(\mu+\upsilon)}\right)\frac{2UV}{4\Delta\eta\Delta\tau}$$

$$\left. + \left(Ge^{-i\upsilon} - G - 1 + e^{i\upsilon}\right)\frac{U^2}{\Delta\tau^2}\right\}$$

$$- \alpha_1\left\{\left(G - Ge^{-i\mu} - 1 + e^{-i\mu}\right)\frac{U}{\Delta\eta\Delta\tau}\right.$$

$$\left. + \left(G - Ge^{-i\upsilon} - 1 + e^{-i\upsilon}\right)\frac{V}{\Delta\tau^2}\right\} = q^2 \cdot \text{L.O.T.} \tag{E12}$$

where

$$\alpha_1 = q^2\left(\frac{\alpha\Delta\tau}{q\Delta t}\right)$$

What is the form to be used for $\alpha\Delta\tau/q\Delta t$? Condition (25) indicates that we use

$$\frac{\alpha\Delta\tau}{q\Delta t} = \frac{Q|U|}{q^2}$$

where $Q^2 > M_L^2 - 1$; therefore $Q = M_L$ is taken for the analysis and so

$$\frac{\alpha\Delta\tau}{q\Delta t} = \frac{M_L\,|U| + 0.1}{q^2} \tag{E13}$$

is sufficient.

Ignoring the L.O.T., since they vanish as $\Delta\eta, \Delta\tau \to 0$ using $\Delta\eta/\Delta\tau = 1$, and taking various values for M_L, U, V, μ and υ, |G| is then calculated from (E12). The computer program to calculate |G| is shown at the end of this appendix. Using the form (E13) it was found that |G| was less than unity when $M_L = 1.001$ but at $M_L = 1.834$ and higher Mach numbers many of the |G| values were greater than unity. Thus an additional ϕ_{St} which is proportional to M_L^2 is indicated and so we next used

$$\frac{\alpha\Delta\tau}{q\Delta t} = M_L^2 \tag{E14}$$

and found $|G| < 1$ in all cases.

On using the form (E14) in the relaxation program it was found that all cases did not converge — presumably due to boundary conditions or to the simplified model used in the above analysis. In fact in the relaxation program it was found necessary to use

$$\frac{\alpha\Delta\tau}{q\Delta t} = M_L^2\left[5 + \frac{5}{0.3}(M - 1)\right]$$

to ensure convergence in the majority of cases. However, for values of M close to 1 and with a fine grid, convergence was sometimes not achieved to sufficient accuracy. For example Table 1 shows the convergence history for $M = 1.02$. The lack of convergence in the latter cases is probably due to the 'cutoff' line AB (Fig. 1) lying partially in the subsonic part of the flow field.

It may be of interest to note that

$$\frac{\alpha\Delta\tau}{q\Delta t} = \frac{M_L^2\,|U| + 0.1}{q^2}$$

gives $|G| < 1$ always but this form has not been tried in the relaxation program.

```
C
C          PROGRAM TO CALCULATE THE AMPLIFICATION FACTOR GIVEN BY
C             FORMULA (E12) USING ALPHA GIVEN BY (E14).
C
C
      COMPLEX ZI,ENU,EMU,EMNU,EMMU,T1,GNUM,GDEN
      REAL*4 MU,NU
      IKN=0
      DMAX=0.
      R=1.
      R2=R*R
      N=5
      N1=N+1
      DMACH=5./N1
      AL=1.01
      PI=3.14159265
      ZI=(0.,1.)
6     XM=1.001
5     XM2=XM*XM
      Q2=7./(1.+5./XM2)
      DQ2=Q2/N
      IKN=0
      KKN=0
      DMAX=0.
      C=SQRT(C2)
      U2=-DQ2
      CNEM=1.-XM2
4     U2=U2+DQ2
      V2=Q2-U2
      U=SQRT(ABS(U2))
      V=SQRT(ABS(V2))
      UV=U*V
      DNU=PI/N
      DMU=PI/N
      MU=1.E-4
      DO 2 J=1,N1
      NU=1.E-4
      DO 1 I=1,N1
      KKN=KKN+1
      AL1=Q2*XM2
      ENU=CEXP(ZI*NU)
      EMNU=1./ENU
      EMU=CEXP(ZI*MU)
      EMMU=1./EMU
      T1=V2*(EMNU*EMNU-2.*EMNU+1.)+2.*UV*R*(1.-EMNU-EMMU+EMNU*EMMU)
     X   +U2*R2*(1.+EMMU*EMMU-2.*EMMU)
      T1=T1*CNEM+U2*(ENU-1.)-0.5*UV*R*ENU*(EMU-EMMU)
      GNUM=T1-AL1*(U *R*(EMMU-1.)+V *(EMNU-1.))
      T1=U2*(EMNU-1.)+V2*R2*(EMU-2.+EMNU)-0.5*UV*R*EMNU*(EMMU-EMU)
      GDEN=-T1+AL1*(U *R*(1.-EMMU)+V *(1.-EMNU))
      D1=CABS(GNUM)
      D2=CABS(GDEN)
      D=D1/D2-1.
      IF(D.GT.0.) IKN=IKN+1
      IF(D.GT.DMAX) DMAX=D
100   FORMAT(11E12.4)
1     NU=NU+DNU
2     MU=MU+DMU
      IF(U2.GT.Q2-1.E-3) GO TO 7
      GO TO 4
7     PRINT 103,XM,IKN,KKN,DMAX
103   FORMAT(/' MACH NO',F6.3,'  NO OF G GREATER THAN 1',I12,
     X   '      TOTAL COMPUTATIONS OF G',I12,
     X   '  MAX G-1',E12.4)
      XM=XM+DMACH
      IF(XM.LT.10.01) GO TO 5
      STOP
      END
```